

**Development of Web-Based Real Time Virtual
Model Based Simulation Laboratory for Soil-
Structure Interaction Problems**

Development of Complete Laboratory Module

Dr. Ali Abolmaali,
Principal Investigator
Award # 0231404

ACKNOWLEDGEMENTS

The investigators are grateful for the financial support from National Science Foundation (NSF), Award # 0231404.

ABSTRACT

A 3-D Web-based non-linear semi-rigid frame analysis program is developed to incorporate the geometric and material non-linearity using C# (C-sharp) .NET programming language. The concept of hybrid element with attaching pseudo spring representing the flexural connection and plasticity effect are employed to modify the element stiffness matrix of the beam. This stiffness modification is related to the connection spring stiffness and/or section yielding at each beam ends. The kinematic hardening model is used in the implementation of connection spring stiffness in non-linear analysis while the concept of section assemblage method presented by Chan and Chui (1997) is employed for evaluating the effect of section yielding. With the matrix condensation method and the reduction form of element stiffness, the effect of these non-linearity are directly included in the beam element stiffness without the addition DOFs need. The non-linear procedures have been performed based on the Newton-Raphson method in which the tangent stiffness is used. To visualize the results in 3-D, the program is performed to represent the input and output geometry graphically in oblique projection viewing.

TABLE OF CONTENTS

ACKNOWLEDGEMENTS.....	iv
ABSTRACT	v
LIST OF ILLUSTRATIONS.....	xi
LIST OF TABLES.....	xiv
Chapter	
I INTRODUCTION AND BACKGROUND	1
1.1 Introduction	1
1.2 Literature Review.....	3
1.2.1 Semi-Rigid Connection	3
1.2.2 Static Plastic Analysis.....	5
1.3 Goals and Objectives.....	7
II BACKGROUND ON NONLINEAR FRAME ANALYSIS AND STEEL CONNECTION	8
2.1 First-Order Linear Elastic Analysis.....	8
2.2 Second-Order Non-linear Elastic Analysis.....	9
2.2.1 The $P - \delta$ effect	11
2.2.2 The $P - \Delta$ effect.....	11
2.3 Second-Order Non-linear Inelastic Analysis.....	12
2.3.1 Concentrated plasticity approach.....	13
2.3.2 Distributed plasticity approach.....	14

2.3.3 Refined-plastic hinge method	14
2.4 Non-linear Solution Method Used: Newton-Raphson Method	22
2.5 Behavior of Connections	23
2.6 Classifications of Connections	25
2.7 Type of Semi-Rigid Connections	26
2.8 Connection Model Used: Kinematic hardening method	29
III INTRODUCTION OF 3-D WEB-BASED IMPLEMENTATION IN C#.....	33
3.1 Introducing C# Web Application.....	33
3.1.1 Introducing .NET	33
3.1.2 The .NET framework and common language runtime	34
3.1.3 Introducing C#	36
3.2 3-D Graphics.....	36
3.2.1 Parallel projections	37
3.2.2 Perspective projections	41
IV FINITE ELEMENT FORMULATION AND PROGRAM IMPLEMENTATION	45
4.1 Coordinate Systems and Transformation Matrix.....	45
4.1.1 The global coordinate system	45
4.1.2 The local coordinate system	46
4.1.3 The transformation matrix	47
4.2 Element Stiffness Formulation	51
4.3 Tangent and Geometric Stiffness Formulation.....	56

4.4 Modified Element Stiffness Accounting for Effects of Joint Flexibility and Material Yielding	58
4.4.1 Hybrid element with connection spring.....	58
4.4.2 Modified element stiffness matrix accounting for Semi-rigid joints.....	59
4.4.3 Modified element stiffness matrix accounting for Material yielding	64
4.4.4 Modified element stiffness matrix accounting for Semi-rigid joints and material yielding.....	67
4.5 Program Algorithm.....	70
4.5.1 Linear elastic analysis.....	70
4.5.2 Nonlinear elastic and inelastic analysis by Newton-Raphson method.....	71
V PROGRAM VERIFICATIONS.....	74
5.1 Program Algorithm Verifications.....	74
5.2 Semi-Rigid Connection Parameters.....	76
5.3 Behavior of Semi-rigid Connections in Linear Analysis.....	77
5.4 Behavior of Semi-rigid Connections in non-linear analysis.....	78
5.5 Web-Based Representation.....	80
VI SUMMARY, CONCLUSION, AND RECOMMENDEDATION.....	92
6.1 Summary.....	92
6.2 Conclusion.....	93
6.3 Recommendation.....	93

Appendix

A. FINITE ELEMENT ANALYSIS	95
B. GRAPHICAL INTERFACE INPUT VERIFICATION.....	187
C. 3-D GRAPHICAL IMAGE	262
D. TABULATED OUTPUT	303
REFERENCES	337
BIOGRAPHICAL INFORMATION.....	339

LIST OF ILLUSTRATIONS

Figure	Page
2.1 General analysis types for framed structures[1]	9
2.2 The $P - \delta$ and $P - \Delta$ effect[1].....	11
2.3 Diagrammatic moment-curvature relationship[1].....	13
2.4 AISC-LRFD bilinear strength curve (AISC-LRFD, 1986)[1]	16
2.5 The section assemblage concept[1]	17
2.6 First yield and full yield surfaces of section[1]	19
(UB356 x 171 x 67 kg/m determined by the present theory)	
2.7 Conventional Newton-Raphson method	22
2.8 Modified Newton-Raphson method.....	23
2.9 Rotational deformation of a connection.....	24
2.10 Connection moment-rotation curves	25
2.11 Common type of beam-column connections.....	27
2.12 Kinematic hardening model	31
3.1 Compilation step in the transition from source code to executable code	35
3.2 Classification of projection	37
3.3 Parallel projection defined by the Center of Projection (PRP) placed at an infinite distance from the view plane	38
3.4 Direction of projectors for an orthographic projection	39
3.5 Orthographic projection	39

3.6	Direction of projectors for an oblique projection.....	40
3.7	Conversion of 3D coordinate point to the view plane for an oblique projection	40
3.8	Oblique projection.....	41
3.9	Pyramidal view volume for a perspective projection.....	42
3.10	Perspective projection.....	42
3.11	One-point perspective projection	44
3.12	Two-point perspective projection.....	44
4.1	The global coordinate system.....	46
4.2	The local coordinate system.....	47
4.3	Definition of angles between global and local coordinate system	48
4.4	Successive rotation method[2]	49
4.5	Two dimensional beam member]	51
4.6	Bending in two planes.....	52
4.7	Column spring element[1].....	58
4.8	Deformed beam-column element with connection sprints[1].....	59
4.9	Two spring-in-series hybrid element[1].....	67
4.10	Deformed beam-column element with 2 spring-in-series.....	68
5.1	Example Frame 1	74
5.2	Example Frame 2	75
5.3	Load-displacement curves in linear analysis of Frame 1(Fig. 5.1)	77
5.4	Load-displacement curves in linear analysis of Frame 2(Fig. 5.2)	78

5.5	Load-displacement curves in non-linear analysis of Frame 1(Fig. 5.1)	79
5.6	Load-displacement curves in non-linear analysis of Frame 2(Fig. 5.2)	80
5.7	Node and element numbering of Frame 2 (Fig. 5.2) for web-based example	81
5.8	Initial geometry of Frame 2 for Web-based example	85
5.9	Deform geometry of Frame 2 for Web-based example in Nonlinear inelastic semi-rigid analysis	86

LIST OF TABLES

Table	Page
2.1 Empirical Equations for Shape Parameter n	31
5.1 Material properties parameters used in the program verification	76
5.2 Semi-rigid connection parameters used in the program verification	76
5.3 Node input of Frame 2 for Web-based example	82
5.4 Element input of Frame 2 for Web-based example.....	82
5.5 Load input of Frame 2 for Web-based example.....	83
5.6 Connection parameter input of Frame 2 for Web-based example.....	83
5.7 Yielding parameter input of Frame 2 for Web-based example.....	84
5.8 Deformed geometry in non-linear elastic analysis of Frame 2 with rigid connections.....	87
5.9 Member forces in non-linear elastic analysis of Frame 2 with rigid connections.....	88
5.10 Deformed geometry in non-linear elastic analysis of Frame 2 with Top- and Seat-angle connections.....	89
5.11 Deformed geometry in non-linear inelastic analysis of Frame 2 with rigid connections.....	90
5.12 Deformed geometry in non-linear inelastic analysis of Frame 2 with Top- and Seat-angle connections.....	91

CHAPTER I

INTRODUCTION AND BACKGROUND

1.1 Introduction

In conventional analysis and design of steel structures, beam-column joints are ordinarily treated as either perfectly rigid or ideally pinned for simplicity. Perfectly rigid connections, as they allow full transfer of moment from beam to column, have been implied that the angle between adjoining members remains unchanged. On the other hand, pinned connections do not transfer moment between adjoining members, but they allow full transfer of shear and axial forces between the beam and the column. The rigid assumption implies that the connection stiffness relative to the beam and connecting column stiffness is large so that the lateral stiffness is provided by the moment action in the frames while the pinned joint assumption considers the joint stiffness to be very small compared with the connected member stiffness and the beams are stanchions only to resist vertical loads. In reality, beam-to-column connections display a nonlinear behavior that lies somewhere between the idealized rigid and pinned conditions. This nonlinearity starts from early stages of loading; the degree of which entirely depends on the geometric parameters of the connection in mechanism.

In engineering analysis, the finite element method (FEM) is the most popular means of simulating engineering systems behavior subjected to static and dynamics loads. FEM is an analytical procedure whose active development has been pursued for a

relatively short period of time. The FEM can be applied to systems with both linear and nonlinear equilibrium equations. Because of simplicity, linear analysis is the most widely used method in practice. Results are only valid for elastic structures with small deformation. When the geometry change is significant or the material yields, non-linear analysis becomes an essential part of structural design. Non-linearity due to beam-to-column connection deformation, member material yielding, and the second-order effects of geometric changes govern the load-carrying capacity of frame structure and need to be considered to improve the accuracy of the results.

To visualize and compare the results of each analysis type, dynamic web-site with ASP.NET have been selected to run programs which are written in C# (C-sharp) language. C# is a full-blown object-oriented visual programming language that adapts the best features of C++ and Java and add new feature of its own. In spite of the limit that .NET Framework exists only for the Windows platform, ASP.NET allows developers to program Web-based applications using .NET's powerful object-oriented languages such as C# and Visual Basic .NET, rather than only scripting languages. In addition, Visual Studio.NET compiles code into the *Microsoft Intermediate Language* (MSIL) which is processor independent and portable with a number of platforms. To compile MSIL code, Microsoft provides a set of Just-in-Time (JIT) compilers for each supported platform. The JIT compiles MSIL code into native machine code, so the JIT compiler is not needed to run the component. The compilation results in the slower method calls the first time the code is run. However, it is compiled to native machine code so that the code performs faster because the JIT compiles the code to machine

code that is specific to the processor running the code. This offers a considerable performance advantage, especially, for the large mathematical program that needs to optimize calculation time for web base application.

1.2 Literature Review

1.2.1 Semi-Rigid Connections

Since the rotational stiffness of beam-to-column joints have been first studied by Wilson and Moore (1917), hundreds of tests have been carried out by many researchers to establish the relationship between moments and relative rotations of beam-to-column connections. Prior to 1950, riveted connections were tested by Young and Jackson (1934) and Rathbun (1936). Using high-strength bolts as structure fasteners was tested by Bell et al. (1958). Subsequently, Sommer (1969) conducted twenty tests to investigate the behavior of header plate connections. Since the late 1960s, flush end-plate and extended end-plate connections for more rigid connections have been used extensively. These 2 types of connections were tested by Ostrander (1970) and Johnstone and Walpole (1981), respectively. Furthermore, Davison et al. (1987) performed a series of tests on a several types of beam-to-column connections and an informative database of connection moment-rotation $M - \phi_c$ curves was collected. More recently, Moore et al. (1993a, 1993b) conducted tests on five full-scale steel frames for the flush end-plate connection, the extended end-plate connection, and the flange cleat connection. The records of member deformation and connections were completely reported, and the results of those were compared with the current British design code BS5950 Part 1 (BS5950, 1990). The extensions and modifications to the existing code

have been proposed to achieve more accuracy of analysis results accounting for joint stiffness.

Extensive research has been carried out in the past few decades to classify the connection types and make the mathematical model of connection stiffness. Frye and Morris (1975) collected data of 145 experimental results from the period 1936 to 1970 and classified seven types of connection test ranging from the weakest single web angle connection to the stiffest T-stud connection. They also modeled the moment-rotation relationship using a polynomial function which was previously applied by Sommer (1969). Ang and Morris (1984) gathered 32 test results during the period 1934 to 1976, which were classified into five types, namely the single web angle, the double web angle, the header plate, the top and seat angle and the strap angle connections. Ramberg and Osgood (1943) modeled the more accurate Ramberg-Osgood function representing the standardized moment-rotation relationship for the five commonly used connection types. In addition, Goverdhan (1984) collected a total of 230 experimental results of moment-rotation curves which were digitized to perform a database of connection behavior. Subsequently, a literature survey of beam-column joints during the period 1951 to 1985 has been conducted by Nethercot (1985). The connection test data and the corresponding moment-rotation curve representations were reviewed. Afterward, Kishi and Chen (1986a; 1986b; 1987a, 1987b) further extended the collection including over 300 test results and classified into seven commonly used connection types. Namely, these are the single/double web-angle, top- and seat-angle with/without double web-angle, extended/flush end-plate and header plate connections. A computerized data bank

program namely the Steel Connection Data Bank (SCDB) was developed to systematically store the database on steel beam-to-column joints. Nowadays; the moment-rotation behaviors and the appropriate analytical model for the seven commonly used connection types can be simply obtained and used in the analysis by tabulate and plot in the SCDB program.

1.2.2 Static Plastic Analysis

Since the early twentieth century, many experiments have been conducted to investigate the strength of beam-column members under various combined axial force and end moment (Johnston and Cheney, 1942; Massonnet and Campus, 1956; Ketter et al., 1952; Ketter et al. 1955; Mason et al., 1958). Based on the experimental data, Galambos and Ketter (1961) established the interaction curves which included the influence of residual stresses on cross-sections for determining the in-plane strength of wide flange beam columns. Subsequently, Duan and Chen (1989a) conducted a unified design interaction equation for steel beam-columns subjected to compression combined with bending moments either about the major axis, the minor axis or with biaxial bending moments. These equations are convenient to manually check the capacity of member.

Because of the accuracy of the results, the plastic zone approach has been employed by many researchers (Chu and Pabarcus, 1964; Alvarez and Birnstiel, 1969; El-Zanaty et al., 1980; Yang and Saigal, 1984; White, 1988; Hsiao et al., 1988; Karamanlidis, 1988; Meek and Loganathan, 1990; Kitipornchai et al., 1990; Kitipornchai and Chan, 1990; and Izzuddin and Smith, 1996a, 1996b) to study the

elasto-plastic structural responses. The results of those experiments are usually considered as the exact or benchmark solutions which are used to verify the accuracy and versatility of developed computer programs. In 1992, Toma and Chen applied the plastic zone method to study the inelastic responses of the frames. Recently, Toma et al. (1995) proposed some benchmark examples from selected useful calibration frames for verification studies.

Because of the cost-effectiveness and accuracy meeting the requirement of practicing engineers, research work on developing and applying the second-order plastic-hinge-based inelastic analysis of steel structure has been extensive in the past two decades. Nedergaard and Pedersen (1985) presented a structural analysis method for space frames accounting for material and geometrical non-linearity. Chen and Powell (1982, 1986) adopted a generalized plastic hinge approach for three-dimensional beam-column members by assuming that the plastic hinge was lumped to the two ends of an element. Next, two simplified methods for inelastic analysis of steel frames including geometric non-linearity has been proposed by King et al. (1992). These are the modified plastic-hinge and the beam column strength approaches. In addition, Liew et al. (1992, 1993) presented a second order refined-plastic hinge analysis method for steel frame design. This method accounts for inelastic stiffness degradation by reducing the modulus of elasticity gradually from the elastic stage to the plastic stage. White (1993) compared several plastic-hinge methods for second-order elasto-plastic analysis of steel frames. Al Mashary and Chen (1991) and Yau and Chan (1994) formulated simplified second-order inelastic analysis procedures of steel frames, in which the

gradual cross-section plastification at the end of elements was modeled by a zero-length pseudo-spring with variable rotational stiffness. Recently, Chen and Chan (1995) conducted an extended pseudo-end-spring model and an efficient method for elasto-plastic large-deflection analysis of steel frames under uniformly distributed load by modeling an element with plastic hinges at mid-span and two ends. More recently, Kato et al. (1998) applied the plastic hinge procedure to study the collapse load of semi-rigid reticulated domes.

1.3 Goal and Objectives

The objective of this research is to make advances in the following fronts:

1. To develop a web-based real time structural analysis algorithm for analysis of three-dimensional frame with semi-rigid joints.
2. To develop a web-based real time algorithm to present analysis results graphically with animation capabilities.
3. To develop a coupled nonlinear algorithm for analysis of three-dimensional frames with flexibility joints by considering: (1) material nonlinearity of beam materials; (2) geometry nonlinearity; and (3) beam-to-column connection nonlinearity.

CHAPTER II
BACKGROUND ON NONLINEAR FRAME ANALYSIS
AND STEEL CONNECTION

2.1 First-Order Linear Elastic Analysis

Linear analysis lies in the assumption that the deflection of a structure is assumed to be very small and the second-order effects due to geometrical changes are negligible. This approach assumes the deflection is proportional to the applied load so that the relationship between load and deflection at any point in a structure is a straight line, as shown in Fig. 2.1, which is the line coinciding with the initial slope of any other analysis.

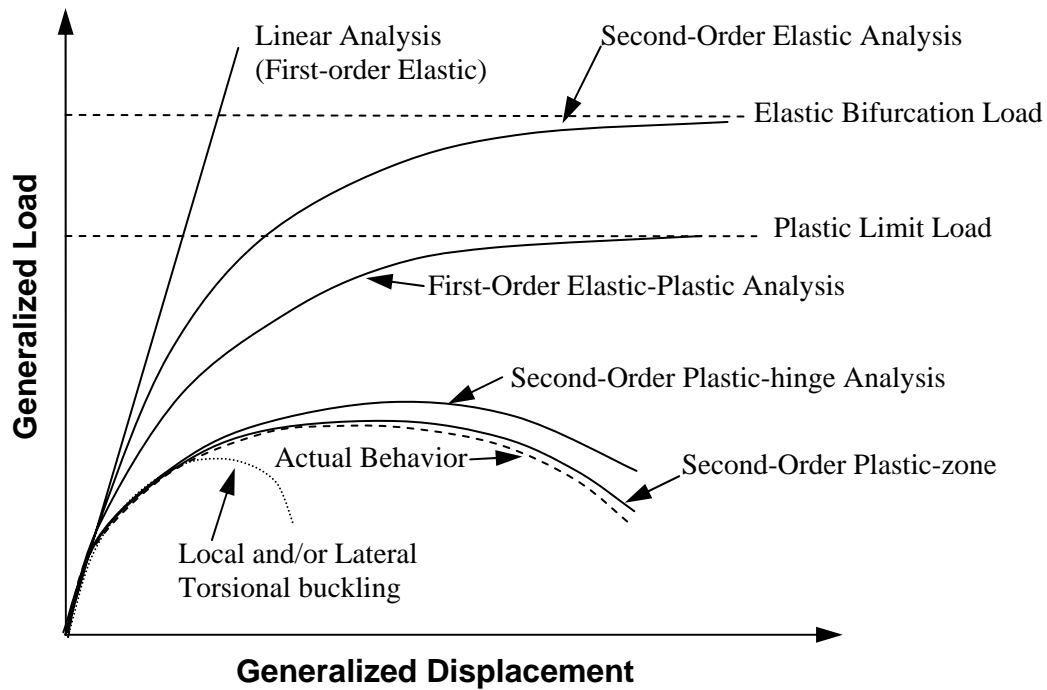


Fig. 2.1 General analysis types for framed structures[1]

Linear analysis gains the advantages of being computationally simple, which is also efficient. A special benefit of the linear analysis is the validity of the application of principle of superposition when subjected to multiple load cases. However, because of linearity, the stiffness of the structural member is taken as constant and independent of the presence of axial force. As a result, this linear approximation may not be accurate due to effects of the element and the structural deflections ($P-\delta$ and $P-\Delta$), respectively. Also the effects of material non-linearity including yielding and formation of plastic hinges are ignored in such analysis techniques.

2.2 Second-Order Non-linear Elastic Analysis

Second-order elastic analysis takes into account the second-order effects due to changing of geometry and initial stress in members, which considers the $P-\delta$ and

$P-\Delta$ effects in the analysis. These geometrical nonlinearity effects are particularly important especially for slender structures subjected to high gravity loadings and their existence as illustrated in Fig. 2.2. Because the structural response is affected by the interaction between loads and deformations, the superimposition technique is not valid for a non-linear analysis.

When allowing second-order effects due to a change in geometry by incorporating the variation of element stiffness in the presence of axial force, the calculated deflections, forces, and moments will be more accurate than the linear analysis. However, as implied by its name, effect of material yielding is not included in the second-order elastic analysis, which allows this method to over-predict the collapse load of a structure. As shown in Fig. 2.1, the load-deflection curve for second-order elastic analysis follows the exact linear equilibrium path before yielding, and then it deviates and becomes nonlinear due to geometric nonlinearity. In addition, because the stiffness of structure is dependent on the axial force in the members, formation of stiffness matrix depends on the displaced configuration of the structure that is not known in advance. As a result, the second-order analysis method can only be performed by an iteration process.

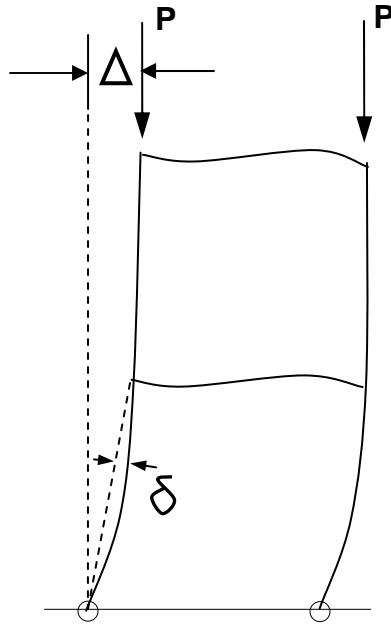


Fig. 2.2 The $P - \delta$ and $P - \Delta$ effect[1]

2.2.1 The $P - \delta$ Effect

The $P - \delta$ effect is referred to as the geometrical nonlinearity effect due to the deflection along a member and the axial force. This force tends to reduce the flexural rigidity of the member, in the other words; the presence of axial force in a member is detrimental to the strength of the member. This $P - \delta$ effect can be included in analysis by the use of *stability stiffness functions* in a beam-column formulation or by the use of a *geometrical (or initial stress) stiffness matrix* in a finite element formulation.

2.2.2 The $P - \Delta$ Effect

If the $P - \Delta$ effect is to be considered in a structural analysis, the original geometry can no longer be applied for the formulation of the transformation matrix because of the change in coordinates. The geometry of a structure can be updated by the updated Lagrangian formulation as

$$x_{i+1} = x_i + u_i \quad (2.1)$$

where x_i and u_i are the coordinates and deflections at the i^{th} loadstep, respectively. The transformation matrix is then updated based on this new geometry, thus, the effect of large deflection is included.

2.3 Second-Order Non-linear Inelastic Analysis

In second-order analysis, nonlinearities in structures exist in two forms: geometry nonlinearity and material nonlinearity. If the effect of material nonlinearity or material yielding is included in the analysis, it becomes the second-order inelastic analysis. Material yielding considerably affects the ultimate load capacity of most structures. Fig. 2.3 represents a moment-curvature relationship for three commonly used types of steel cross-section.

For steel frame structures, material nonlinearity arises when yielding spreads through the member cross-section (plastification) and along the member length (plastic zone) while the moment in the cross-section increases gradually from the initial yield moment M_y at the outermost fiber to the fully plastic moment M_p . Depending on the level of accuracy required, the inclusion of material non-linearity can be conducted by two approaches, *concentrated plasticity (plastic hinge or lump) approach* and *distributed plasticity (plastic zone) approach*. The first approach simulates the progressive cross-section yielding at the member ends while the latter approach models the spreading of plasticity within the whole volume of the structure. Furthermore, to obtain a more accurate full-yield strength surface of I- or H-sections under moment and axial load, the concept of the central cored web taking axial force and the remaining

area taking moment is established, namely the “*section assemblage approach*”. The brief detail of these two inelastic models and the concept of section assemblage method are introduced in the following sections.

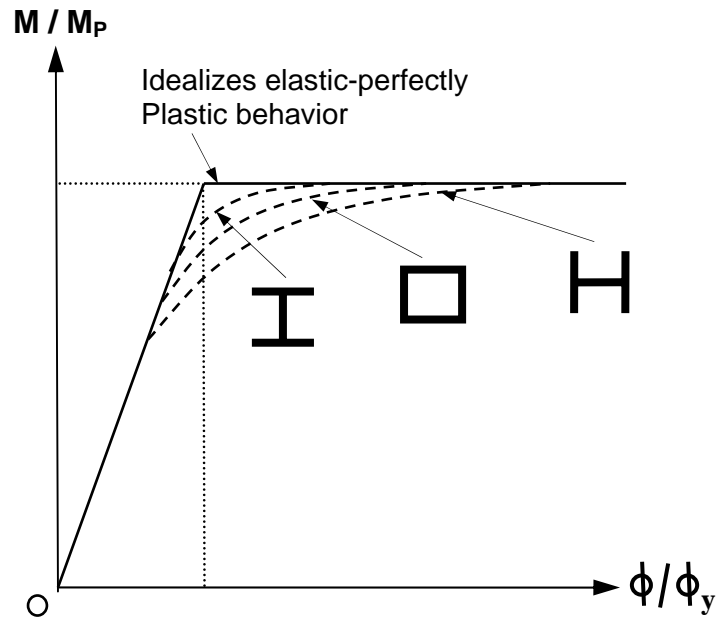


Fig. 2.3 Diagrammatic moment-curvature relationship[1]

2.3.1 Concentrated Plasticity Approach

The Concentrated Plasticity Approach, also referred to as the plastic hinge method, ignore the progressive yielding that takes place along the member length. The basis of this approach is cross-section plastification, where plasticity is assumed to be lumped only at two ends of elements through the use of zero-length spring elements in computer analysis. In this approach, the portion of the member length from the end is assumed to remain elastic throughout the analysis. The commonly used plastic hinge

methods are elastic-plastic hinge method, column tangent modulus method, beam-column stiffness degradation method, beam-column strength degradation method, and end-spring method.

2.3.2 Distributed Plasticity Approach

The Distributed Plasticity Approach or plastic zone method is a more sophisticated method that takes into account the spread of yielding in the cross-section and along the member length. The procedure is to divide each member into many small elements longitudinally and transversely so that monitoring of stress and strain is carried out for all members. As a result, physical attributes such as initial imperfections and residual stresses can be explicitly included in the analysis by assigning a stress for each sub-area before loading. Because the fundamental stress-strain relationship is directly applied for moments and forces computation, this approach is more accurate than concentrated plasticity approach and, moreover, the results are generally regarded as the exact solutions. However, the plastic zone method is suitable only for simple structures due to huge computational effort required. The commonly used plastic zone methods are traditional plastic zone method and simplified plastic zone method.

2.3.3 Refined-Plastic Hinge Method

In most elasto-plastic analysis, a simplified linear interaction equation is applied to monitor the yielding of a section; in other word, to control the formation of a plastic hinge. However, this linear function is based on the simple combined stress equation for elastic analysis. Thus the function is correct for first yield analysis and can only give an approximation when used in plastic analysis. Researcher such as Chen and Lui (1991)

developed various equations to formulate the ultimate section capacity (AISC-LRFD, 1986) is of the following form:

$$\frac{P}{P_y} + \frac{8}{9} \frac{M}{M_p} = 1.0 \quad \text{for } \frac{P}{P_y} \geq 0.2$$

$$\frac{P}{2P_y} + \frac{8}{9} \frac{M}{M_p} = 1.0 \quad \text{for } \frac{P}{P_y} < 0.2$$
(2.2)

where; $P_y = \sigma_y A$ and $M_p = \sigma_y Z_p$. The definitions for P_y , M_p , σ_y , A , Z_p , P , and M are given as:

P_y = the squash load of the cross-section,

M_p = the plastic moment capacity for member under pure bending action,

σ_y = the yield stress of material,

A = cross-sectional area,

Z_p = plastic modulus,

P, M = axial force and bending at the cross-section being considered.

The bilinear strength curve of these equations, are shown in Fig. 2.4. This empirical formula provides a reasonable lower-bound fit to a general section bent about their principal axes; however, it becomes uneconomical for many other sections. Furthermore, bilinear function leads to an abrupt change of yield function at $P = 0.2P_y$; therefore, represents a discontinuity or kink in the axial force-bending moment curve.

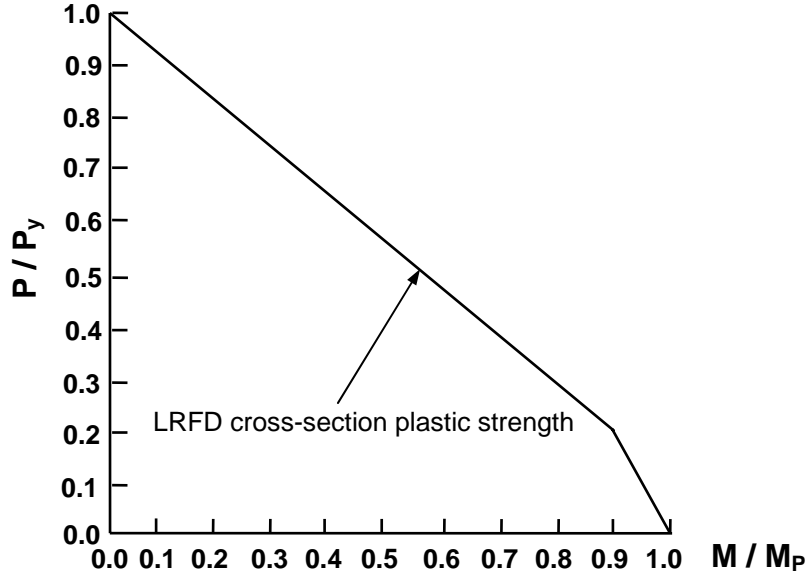


Fig. 2.4 AISC-LRFD bilinear strength curve (AISC-LRFD, 1986)[1]

A more accurate plastic hinge function can be obtained by dividing a section into many small sub-areas and then applying the axial and residual stress as the first initial stress for the sub-areas in the section. This will result in gradual increase of the curvature so that the final strain is computed and the moment versus curvature curves can be generated. Subsequently, the mathematical functions can be formulated these curves and then can be applied to curve fit relationship and collected in a data bank for elasto-plastic analysis. However, despite its accurate, this approach is too complicated for general used and difficult to check by manual approach.

2.3.3.1 The Full and Initial Yield Surfaces By Section Assemblage Method[1]

Section assemblage method has been adopted by Chan and Chui (1997) on the basis of plate assemblage in section. This method assumed that the web takes the axial force and the remaining unyielded area resists the moment. By this concept, the yield functions for both first yield and fully-plastic yield surfaces can be obtained through a

data bank for sectional properties containing the dimensions of flange and web thickness. These functions can be applied to all sections and empirical parameters of yield function such as Eq. 2.2 are not required.

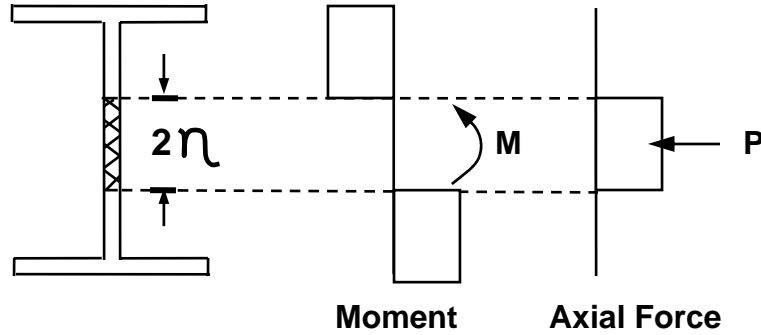


Fig. 2.5 The section assemblage concept[1]

Fig. 2.5 illustrates this concept for I and H sections. For annealed sections with no residual stress, the plastic zone for axial force resistance can be calculated as

$$\eta = \frac{P}{2\sigma_y t} \quad \text{for } \eta \leq \frac{d}{2} \quad (2.3)$$

$$\eta = \frac{(P - \sigma_y t d)}{2B\sigma_y} + \frac{d}{2} \quad \text{for } \frac{d}{2} < \eta \leq \frac{d}{2} + T$$

where P = axial load;

η = half-depth of yielded area for axial load;

σ_y = yield stress;

B = flange width;

t = web thickness;

T = flange thickness;

d = depth of web.

Related to calculated plastic zone in the section, the section moment resistance by the remaining unyielded zones can be obtained as

$$M_{pr} = \left[BT(D-T) + \left(\left(\frac{D}{2} \right)^2 - \eta^2 \right) t \right] \sigma_y \quad \text{for } \eta \leq \frac{d}{2}$$

$$M_{pr} = \left[\left(\frac{D}{2} \right)^2 - \eta^2 \right] B \sigma_y \quad \text{for } \frac{d}{2} < \eta \leq \frac{d}{2} + T$$
(2.4)

where, M_{pr} = reduced plastic moment capacity of section in the presence of axial force;

D = the total depth of section.

As shown in the above equations, section assemblage approach uses only the basic sectional parameters, e.g., the depth, flange width, web and flange thickness, to determine ultimate section strength. The section strength equations are formulated by the interaction relationship between axial force and bending moment. This concept can be applied to many typical sections including rectangular hollows, channel and I-sections. This approach have more advantage in comparing with the existing approach which applies bi-linear full-yield surfaces or artificially shapes of yield surface based on curve-fitting that require a new mathematical curve-fitting for a new different sectional type to generate a new set of mathematical parameters. This section assemblage method is convenience and more consistent and rational than other existing methods and then was selected to used in this thesis. To illustrate this procedure, curves of first yield and plastic moment enveloped are plotted graphically as shown in Fig. 2.6.

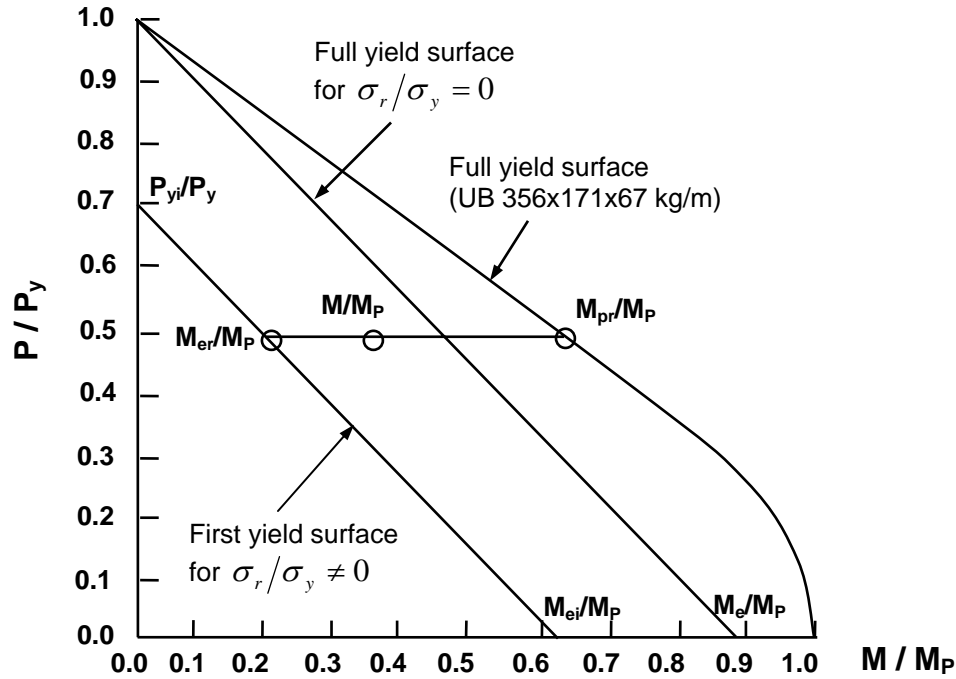


Fig. 2.6 First yield and full yield surfaces of section [1] (UB356 x 171 x 67 kg/m determined by the present theory)

When the axial force-moment lies inside the first yield envelope, the section remains elastic. On the other hand, if the axial force-moment lies outside the full yield surface, the section spring stiffness will be reduce to zero as the moment resistance is set to the plastic moment, and then the unbalance moment will be redistributed in the structure before a mechanism is formed. In elastic-plastic hinge analysis, these two conditions are applicable by defining the first yield and the yield envelopes to coincide. If elasto-plastic hinge analysis is used, the section spring is required to reduce gradually and then this state occurs when the M - P coordinate lies between the first yield and the full yield surfaces. In the existence of axial force and residual stress, the first yield surface can be calculated by

$$M_{er} = \left(\sigma_y - \sigma_r - \frac{P}{A} \right) Z_e \quad (2.5)$$

where M_{er} = reduce first yield moment;

P = axial force;

σ_r = maximum residual stress;

A = cross-section area;

Z_e = elastic modulus.

2.3.3.2 Refined-Plastic Hinge Method Based on the Section Assemblage Concept[1]

To overcome the defect of an abrupt change from ideally elastic to perfectly plastic states, a refined-plastic hinge method is adopted by Chan and Chui (1997). This method conducts a more accurate load-deformation curve of structure and provided a smooth transition of material yielding. Including the effect of residual stress, the first and full yield surfaces are determined. Fig. 2.6 shown the distribution of residual stress which is assumed to be dependent on the depth/flange width ratio. The elastic and plastic moments at given axial load level will be computed and used for the calculation of the section spring stiffness, as the following form:

$$S_s = \frac{6EI}{L} \frac{|M_{pr} - M|}{|M - M_{er}|} \quad \text{for } M_{er} < M < M_{pr} \quad (2.6)$$

where EI = flexural rigidity;

L = member length;

M_{er} = reduced first yield moment; and

M_{pr} = reduced plastic moment.

In this equation, the section stiffness varies from infinity to zero which represents the two extreme values of elastic and plastic moment. When the moment is less than first yield moment, the stiffness of the section spring is infinity, which represents complete transfer of moment from one side to another side of the spring element. On the other hand, when the moment is equal to plastic moment, the spring stiffness is zero, indicating no further moment is transferable across the spring element. Between these two values, the stiffness of spring element is a finite value representing the degree of cross-sectional plastification at the element end.

2.3.3.3 *The Elastic-Plastic Hinge method Based on the Section Assemblage Method[1]*

The elastic-plastic hinge method assumes that the material is either perfectly elastic or fully plastic so that the effect of partial yielding is not considered and the stiffness of section spring model is not degraded. Because of neglecting of partial yielding effect, the predicted ultimate load for this method is generally higher than that for the refined plastic hinge method. Based on section assemblage concept, full-yield strength surface can be simply obtained by Equations 2.3 and 2.4. The section remains elastic if the current force point is within this surface, and the section is assumed to form a fully plastic hinge when the force point is on the surface. In computer analysis, a very large value and very small value is assigned to the section stiffness for the elastic (i.e. $M < M_{pr}$) and plastic (i.e. $M = M_{pr}$) case as follows,

$$\begin{aligned}
 S_s &= 10^{+10} EI/L & \text{for } M < M_{pr} \\
 S_s &= 10^{-10} EI/L & \text{for } M = M_{pr}
 \end{aligned}
 \tag{2.7}$$

2.4 Solution Method Used for Non-Linear Analysis: Newton-Raphson Method

The Newton-Raphson procedure is used, which is a combination of direct iterative and incremental method. In this method, the tangent stiffness is reformed at every iteration, as shown in Fig. 2.7. Alternatively, to simplify this method, the tangent stiffness is reformed at only the first iteration which is referred to the modified Newton-Raphson method (refer to Fig. 2.8). In this research, the conventional Newton-Raphson method is used in implementing the computer program for 3-D semi-rigid frame. The algorithm is presented in Chapter 4.

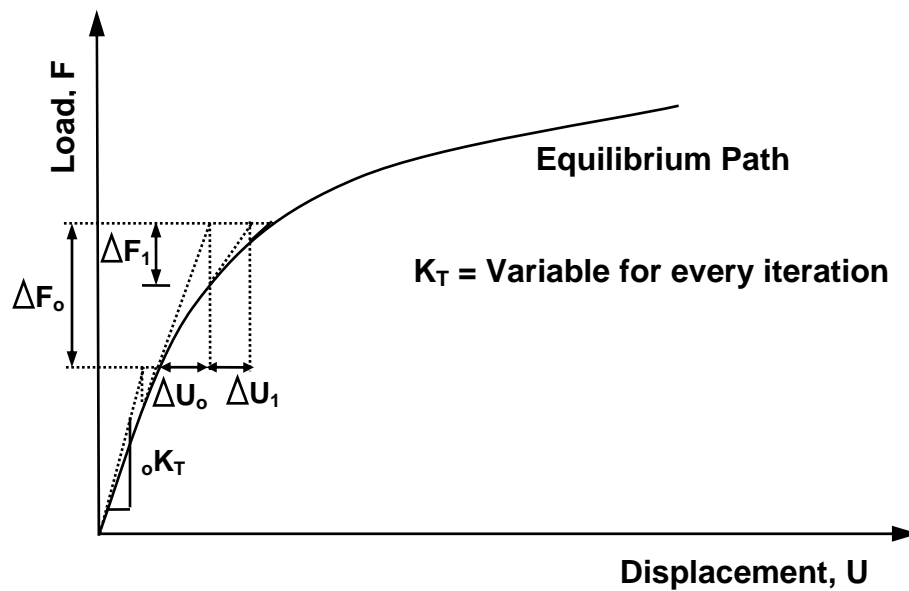


Fig. 2.7 Conventional Newton-Raphson method

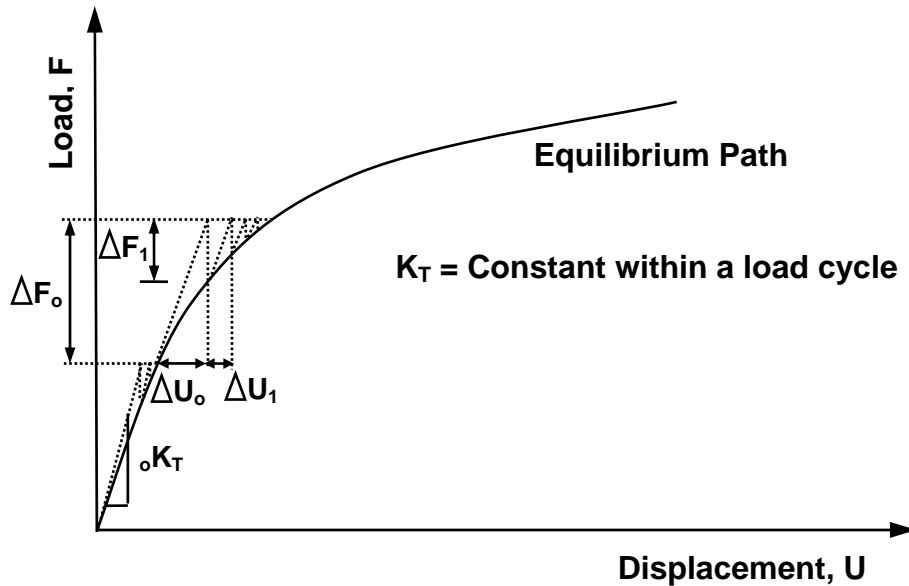


Fig. 2.8 Modified Newton-Raphson method

2.5 Behavior of Connections

A connection is a medium through which forces and moments are transferred from one member to another. In conventional design of steel frames, the connections joining the beams to the column usually assumed to behave as either fully rigid or ideally pinned. As fully rigid assumption, the lateral stiffness is provided by the moment action in the frames such that full gravity moment is transferred from beam to column. On the other hand, the assumption of ideally pinned connection implies that the lateral stiffness is provided by other structural systems such as core or shear wall and an effective bracing system whilst connection only resist vertical load. Although these two assumptions drastically simplify the analysis, in reality the connection behaves neither rigid nor pinned. When a moment M is applied to a connection, it rotates by an amount θ_c as shown in Fig. 2.9. The angle θ_c is a measure of the relative rotation of beam to

column. If the connection behaves rigid (i.e. total moment is transfer from beam to column), then the relative rotation is equal to zero ($\theta_c = 0$).

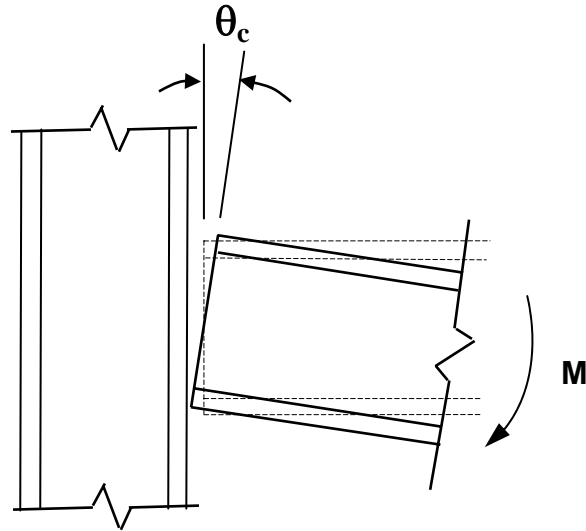


Fig. 2.9 Rotational deformation of a connection

The moment-rotation ($M - \theta_c$) relationships of some commonly used semi-rigid connections are illustrated in Fig. 2.10. As shown in this figure, all types of connections exhibit an $M - \theta_c$ behavior that falls between the two extreme assumptions of ideally pinned (the horizontal axis) and fully rigid (the vertical axis). Furthermore, the $M - \theta_c$ relationships of such connections represent the nonlinear behavior over the entire range of loadings.

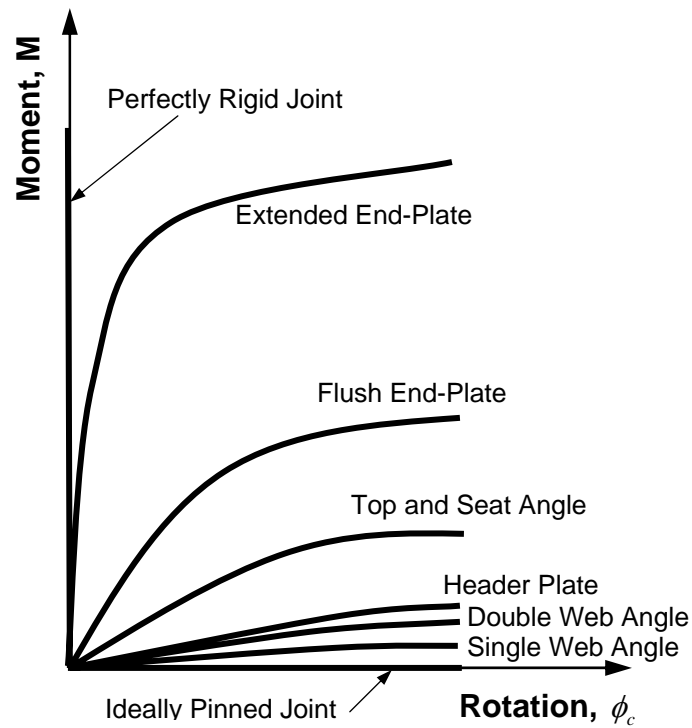


Fig. 2.10 Connection moment-rotation curves

2.6 Classifications of Connections

Recently, semi-rigid behaviors of connections have been recognized and provisions for semi-rigid connections are provided in several national steel design code, such as American Institute of Steel Construction (AISC) in their: (1) Load and Resistance Factored Design (LRFD) Manual (1986), (2) Allowable Stress Design (ASD) Manual (1989). Also these provisions are presented in British Standard BS5950 (1990), Eurocode 3 (1992), and Australian AS4100 (1990). Classification of connections for ASD and LRFD code are as follows:

- 1) ASD Type 1 or “rigid framing”, assumes that the beam-column joints have sufficient rigidity to maintain the original geometric angle between the intersection

members. LRFD specifications designate rigid framing as fully restrained (FR) connections.

- 2) ASD Type 2 or “simple framing”, assumes that only vertical shear reactions are transmitted between connections such that the joints are allowed to rotate without restraint. Simple framing is assumed to exist if rotation between beam and column is approximately 80% or more compared to that for a perfect hinge. LRFD designates such connections as partially restrained (PR) connections.
- 3) ASD Type 3 or “semi-rigid framing”, assumes that the connections can transfer vertical shear as well as be able to transfer some bending moment. This type exists for connections that lie between ASD Type 1 and Type 2 classification. LRFD includes this type of connection as Type PR connections.

Note that in LRFD Specifications, Type FR corresponds to ASD Type 1 and PR includes both ASD Type 2 and 3.

2.7 Type of Semi-Rigid Connections

In this section, common type of connections are discussed. These connections are illustrated in Fig. 2.11 as follow.

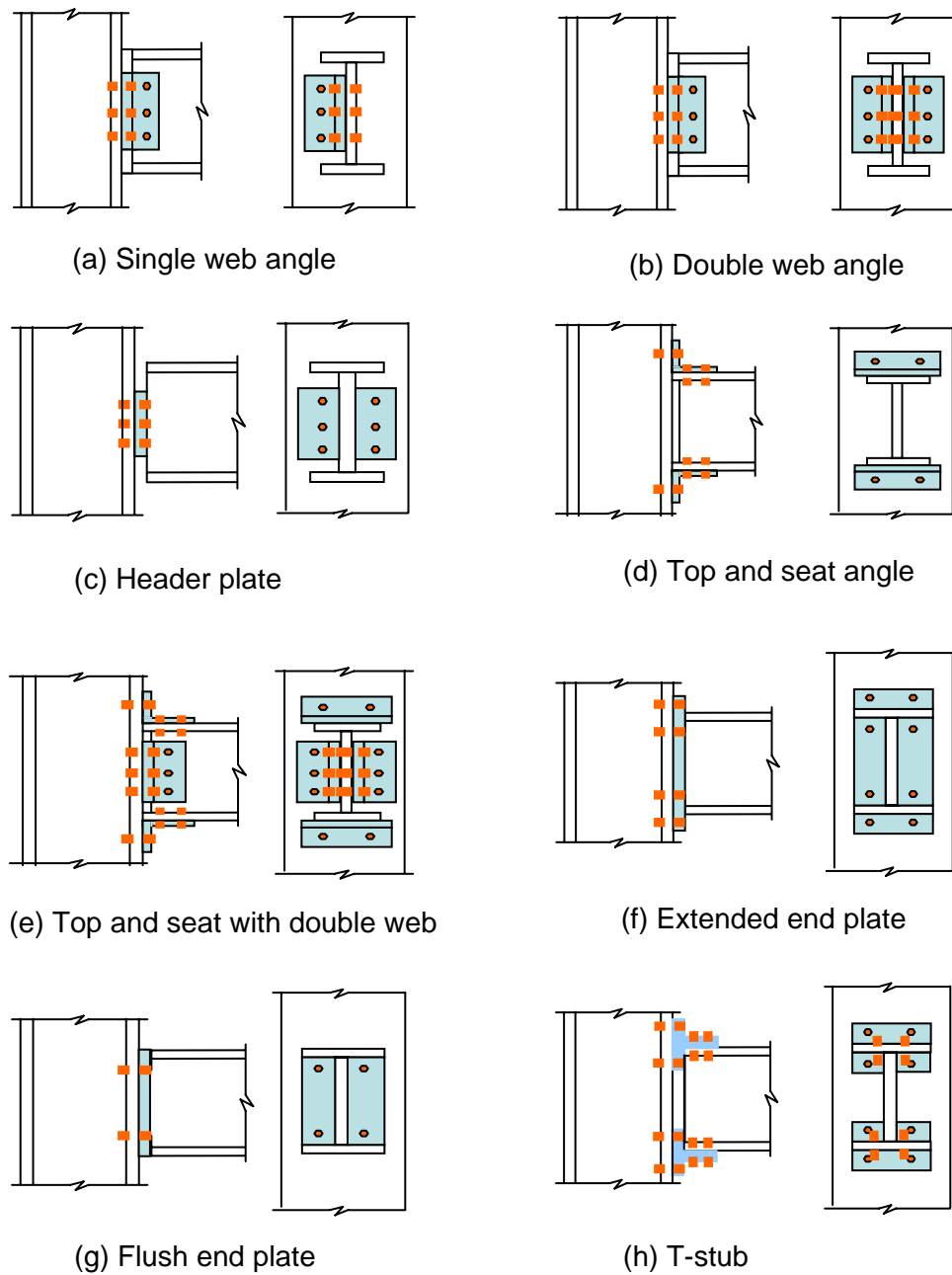


Fig. 2.11 Common type of beam-column connections

Single Web Angle

A single web angle connection consists of an angle either bolted or welded to both column and beam web (refer to Fig. 2.11a). These connections have little moment

rotation rigidity and are very flexible. They would be classified by AISC-ASD Specifications (1989) as Type 2 construction connection (simple connection).

Double Web Angle Connections

Double web angle connection consists of two angles either bolted or welded to both column and beam web (refer to Fig 2.11b). AISC-ASD Specifications (1989) classify this type of connection as Type 2 construction connection (simple connection).

Header Plate Connections

A header plate connection consists of an end plate which its length is less than the depth of beam, welded to the beam and bolted to the column (refer to Fig. 2.11c). The $M - \theta_c$ behaviors of these connections are similar to that of double web angle connection. Also these connections are classified as Type 2 connection.

Top And Seat Angle Connections

As shown in Fig. 2.11d, the AISC-ASD Specifications (1989) define the top and seat angle connection as follow: (1) the seat angle transfers only vertical reaction and should not give significant restraining moment on the end of beam; (2) the top angle is merely for lateral stability and is not considered to carry any gravity loads.

Top And Seat Angle Connections With Double Web Angle

This connection is a combination of top and seat angle and double web angle connection as shown in Fig. (2.11e). By ASD these connections are considered as Type 3 framing connection (i.e. semi-rigid connection).

Extended/flush end-plate connections

The extended end-plate connections are classified into two types as extended end-plate connection either on the tension side only or both the tension and compression sides (refer to Figures 2.11f, 2.11g). These connections are built up by welding the end-plate to the beam end along both flange and web in the fabricator's shop and then bolting end-plate to the column in the field. Both extended and flush end-plate connections are classified as ASD Type 1 framing connection.

T-stub Connections

A T-stub connection consists of two T-stubs bolted to beam and column at the top and the bottom of beam flange as shown in Figure 2.11h. This type of connections is considered as the stiffest ASD Type 3 semi-rigid connections.

2.8 Connection Model Used: Kinematic Hardening Method

Models of moment-rotation behavior of connections can be classify into three types which are an analytical, a mathematical and a mixed model. An analytical model conducts $M - \theta_c$ relationship based on the physical characteristics of a connection. On the other hand, a mathematical model establishes such relationship by a mathematical function in which the parameters are based on the curve-fit test results. As implied by its name, a mixed model combine these two concepts so that the functions are expresses in terms of both curve-fitting constants and geometric parameters. There are several commonly used mathematical and mixed models for representing the $M - \theta_c$ relationships of beam-column connections. In this research, a kinematic hardening model is used. The description of this model is presented in the subsequent paragraph.

The kinematic hardening model (Huang and Morris, 1991) is a modified independent hardening model to take into account the effect of material hardening. Fig. 2.12 represents the $M - \theta_c$ diagram with the hardening line ($M = S_h \phi_c$) having slope S_h . In this model, the reversal unloading path follows the line with the slope of the initial connection stiffness S_c^0 which is line AB or CD until it reaches the hardening line. When the unloading process goes beyond this line, the path follows the virgin non-linear $M - \theta_c$ curve under the monotonic static loading which is curve BC or DE. Therefore, the path of $M - \theta_c$ curve follows the virgin curve earlier comparing to independent hardening method. This method can be formulated as

$$M = S_c^0 \theta_c \left(\frac{1 - S_h / S_c^0}{\left\{ 1 + \left[(1 - S_h / S_c^0) \theta_c / \theta_0 \right]^n \right\}^{1/n}} + \frac{S_h}{S_c^0} \right) \quad (2.8)$$

$$K = \frac{dM}{d\theta_r} = AD + ABE^{(-1/n)} - ABC^n \theta_r^n E^{(n-1-2/n)} \quad (2.9)$$

where, n = shape parameter;

S_h = slope of asymptotic line;

$\theta_0 = \frac{M_u}{S_c^0}$ which is called reference plastic rotation;

$S_c^0 = A$ = initial connection stiffness;

$B = 1 - S_h / S_c^0$

$C = B / \theta_0$

$D = S_h / S_c^0$

$$E = 1 + C^n \theta_c^n$$

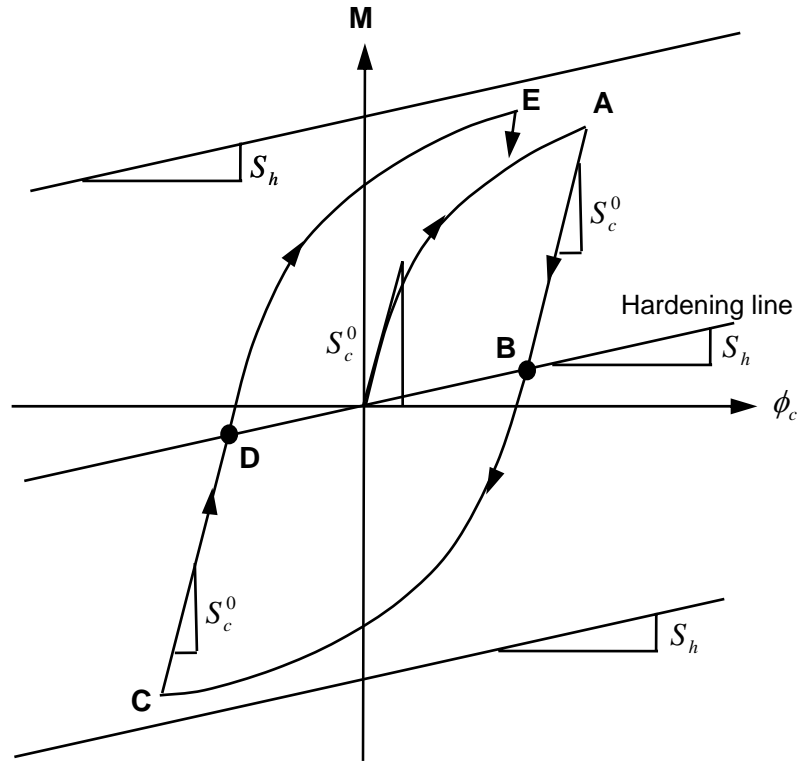


Fig. 2.12 Kinematic hardening model

The shape parameter n can be obtained from the empirical equations as shown in Table 2.1.

Table 2.1 Empirical Equations for Shape Parameter η

Connection Type	η
Single web-angle connection	$0.520 \log_{10} \theta_0 + 2.291$ ($\log_{10} \theta_0 > -3.073$)
	0.695 ($\log_{10} \theta_0 \leq -3.073$)
Double web-angle connection	$1.322 \log_{10} \theta_0 + 3.952$ ($\log_{10} \theta_0 > -2.582$)
	0.573 ($\log_{10} \theta_0 \leq -2.582$)
Top- and seat-angle connection (without double web-angle)	$1.398 \log_{10} \theta_0 + 4.631$ ($\log_{10} \theta_0 > -2.721$)
	0.827 ($\log_{10} \theta_0 > -2.721$)
Top- and seat-angle connection (with double web-angle)	$2.003 \log_{10} \theta_0 + 6.070$ ($\log_{10} \theta_0 > -2.880$)
	0.302 ($\log_{10} \theta_0 \leq -2.880$)

Mathematically, this method is exactly the same as the independent hardening method if S_h equal to zero which is the hardening line coincide with x-axis. Because the kinematic hardening method is convenient and the hardening effect is included, this model is employed to implement the static semi-rigid connection analysis in this current study.

CHAPTER III

INTRODUCTION OF 3D WEB-BASED IMPLEMENTATION IN C#

3.1 Introducing C# Web Application

3.1.1 Introducing .NET

.NET is a set of cross-platform technologies, or in the other words; it is independent from a specific language or platform. This allows any code in the .NET language (such as C#, Visual C++ .NET, Visual Basic .NET and many others) to contribute to the same software project. For example, an application built in VB.NET can inherit from C# class. In addition, .NET incorporates key technologies such as, Microsoft's *Active Server Page* (ASP).NET (Web), Windows forms (Window GUI or *Window Graphic User Interface*), and ADO.NET (data access). These capabilities allow developers using ASP.NET to develop powerful and robust Web applications by taking advantage of ASP. NET's optimizations for performance, testing and security.

.NET Framework is a main part of .NET. This framework manages and executes applications, contains a class library (called the *Framework Class Library*, or FCL), enforces security and provides many other programming capabilities. The .NET framework supports ASP.NET (Active Server Pages) applications which allow programmers to create applications for the Web. With ASP.NET, developers can create Web-based and database-intensive applications quickly by harnessing the power of .NET's object-oriented languages.

Complementing the .NET Framework is Visual Studio.NET, an integrated development environment. Visual Studio .NET provides easy access to server functionality. Designers, including XML Data Designer, Web Services Designer, Windows Forms Designer, and Web Forms Designer, are the key components of Visual Studio .NET. These designers provide simply access to generated code based on class frameworks. The generated code is accessible to the developer, allowing the developer to modify or add code. Furthermore, Visual Studio .NET's Visual Web Page Editor's WYSIWYG (What You See Is What You Get) interface eliminates the need to master HTML by using Web Form Designer which make process to generate the Web application simpler and faster.

3.1.2 The .NET Framework and Common Language Runtime

One significant enhancement to Visual Studio .NET is the addition of a language independent runtime called the *Common Language Runtime* or CLR. CLR provides an execution environment that incorporates features such as memory management, security management, code verification and compilation. The compilation from source code to executable code is summarized in Fig. 3.1.

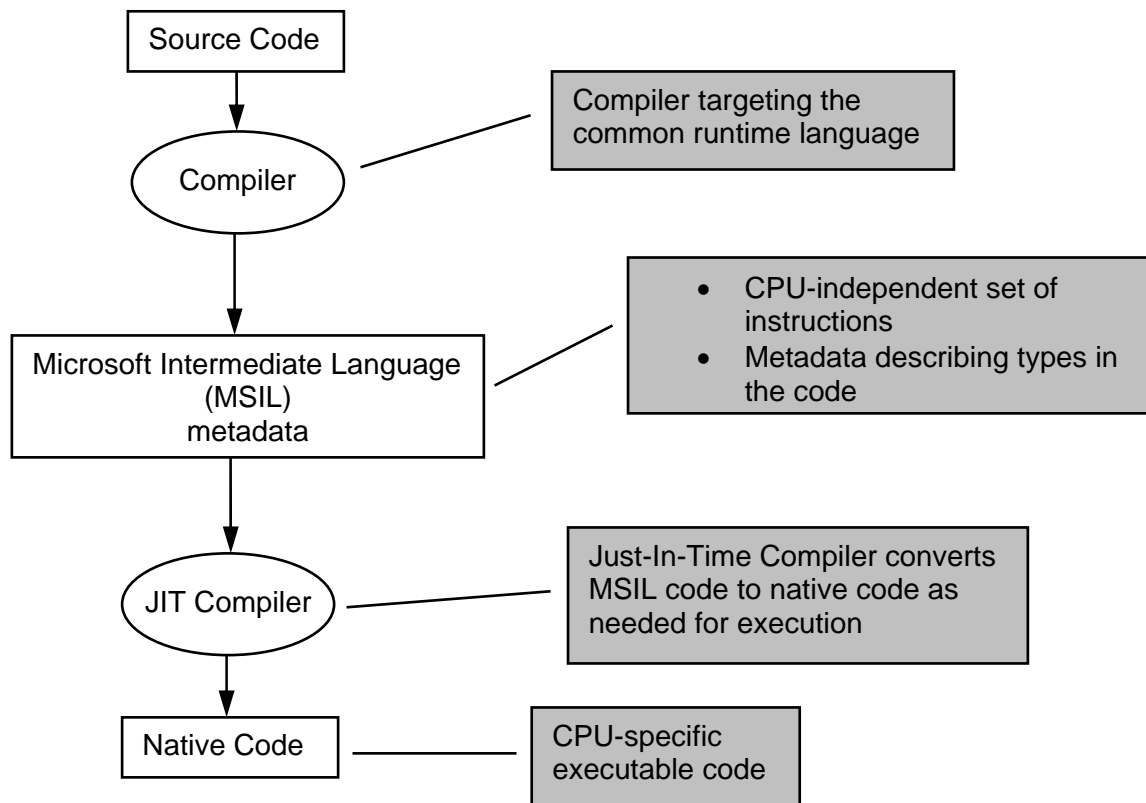


Fig. 3.1 Compilation steps in the transition from source code to executable code

Programs are compiled into machine-specific instructions in two steps. First, the source code is compiled with a compiler targeting CLR so that the code is compiled into Microsoft Intermediate Language (MSIL) which is a CPU-independent set of instructions. The compiler also creates metadata along with the compiler code to provide information about the types, members and references in the code. These metadata are used by the runtime to manage code execution, therefore, eliminating the need for Type Libraries and Interface Definition Language. Then the just-in-time (JIT) compiler, which is supplied for each CPU, compile the MSIL code into native machine code (for a particular platform), creating a single application. In conclusion, the main concept of CLR is the ability to compile once and make the code run on any platform

that supports CLR. Nowadays, the .NET Framework exists only for the Windows platform; however, it is being developed for other platforms.

3.1.3 Introducing C#

The C# (pronounced “C-Sharp”) programming language is a language specifically designed for a .NET platform. C# incorporates the best features of other popular programming languages, such as C, C++, Java, and Visual Basic and adding new features of its own. As a result, C# is an event-driven, fully object-oriented, visual programming language that can create any type of application. C# programs are created using *Integrated Development Environment* (IDE) which allows the programmer to create, run, test, and debug C# programs conveniently, therefore, greatly reducing the time to produce a working program. The process of creating an application rapidly using an IDE is referred to as *Rapid Application Development* (RAD).

3.2 3-D Graphics

To draw any 3D object on computer flat screen that has 2D coordinate system, the first process is to convert 3-dimensional coordinates to 2-dimensional screen pixels, or referred to projection. Projection means turning 3D into 2D, which meaning projecting the real three dimensional object into a plane. Generally, the plane z equal to zero is usually chosen in practice, because it allows working with the remaining x and y coordinates by simply plotting them on the screen.

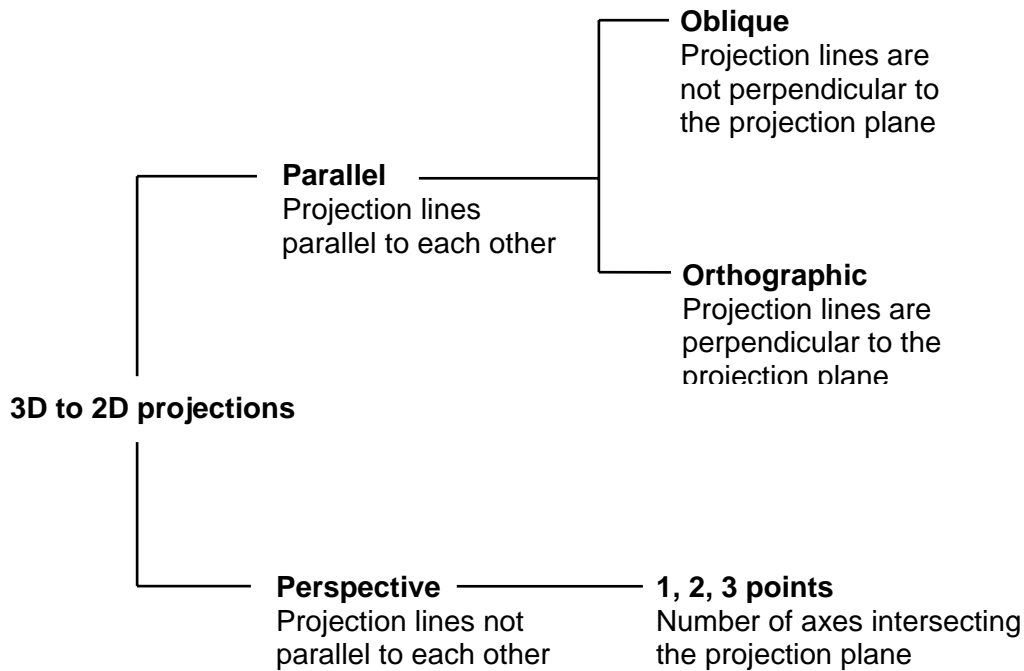


Fig. 3.2 Classification of projection

3.2.1 Parallel Projections

One of the most important characteristics of parallel projections concerns the placement of the center of projection (PRP) which represents the camera or viewing position. In a parallel projection, the camera is located at an infinite distance from the view plane (refer to Fig. 3.3). By placing the camera at an infinite distance from the view plane, projectors to the view plane become parallel which is the second characteristic of a parallel projection. Only objects within the view volume are projected to the view plane. Fig. 3.3 shows the projection of line AB to the view plane. In this case, the measurement of line AB is maintained in the projected line A'B'. While the measurements of an object are not preserved in all parallel projections, the parallel nature of projectors maintains the proportion of an object along a major axis. Therefore,

parallel projections are useful in applications requiring the relative proportions of an object to be maintained, and then is applied in this Web-based applications.

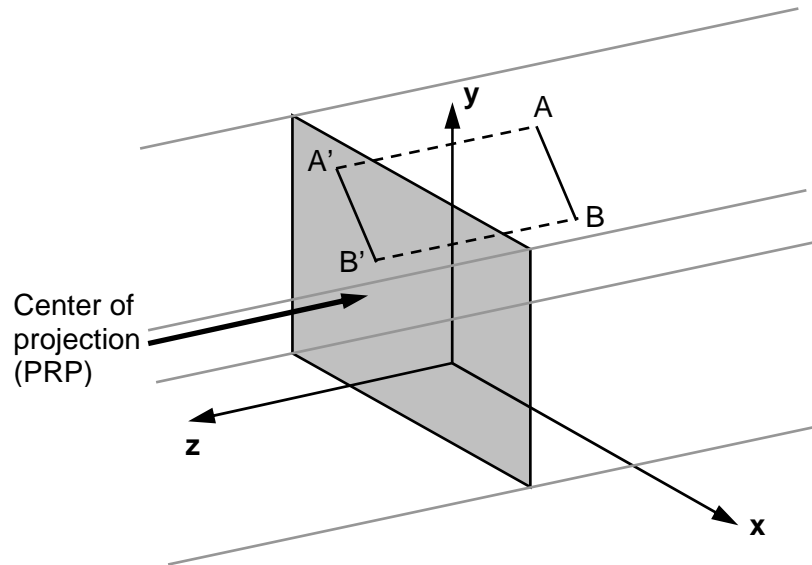


Fig. 3.3 Parallel projection defined by the Center of Projection (PRP) placed at an infinite distance from the view plane

3.2.1.1 Orthographic Parallel Projections

In addition to being parallel, projectors in orthographic projection setting are also perpendicular to the view plane as presented by Hearn & Baker(1996) and as shown in Fig. 3.4.

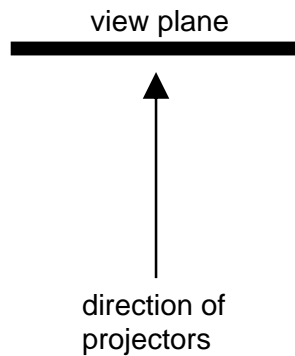


Fig. 3.4 Direction of projectors for an orthographic projection

Mathematically, orthographic projection can be simply implemented by cutting off the z-coordinate for each point in the object. The projection matrix can be expressed as follow,

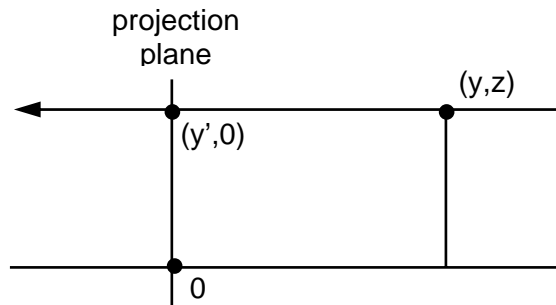


Fig. 3.5 Orthographic projection

$$\begin{bmatrix} x' \\ y' \\ 1 \end{bmatrix} = \begin{bmatrix} x \\ y \\ 1 \end{bmatrix} = \begin{bmatrix} 1 & 0 & 0 & 0 \\ 0 & 1 & 0 & 0 \\ 0 & 0 & 0 & 1 \end{bmatrix} \begin{bmatrix} x \\ y \\ z \\ 1 \end{bmatrix} \quad (3.1)$$

3.2.1.2 Oblique Parallel Projections

Oblique view presents an object's 3D appearance as well as displays the exact shape of one face Hill (1990). As in an orthographic view, Oblique view uses parallel projectors but the angle between the projectors and the view plane is no longer

orthogonal. In the other words, an oblique projection is a parallel projection where the projecting lines are not perpendicular to the projection plane. Fig. 3.6 shows an example of the direction of the projectors in relation to the view plane.

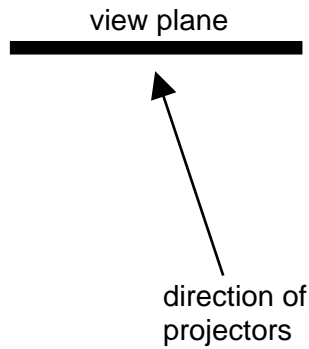


Fig. 3.6 Direction of projectors for an oblique projection

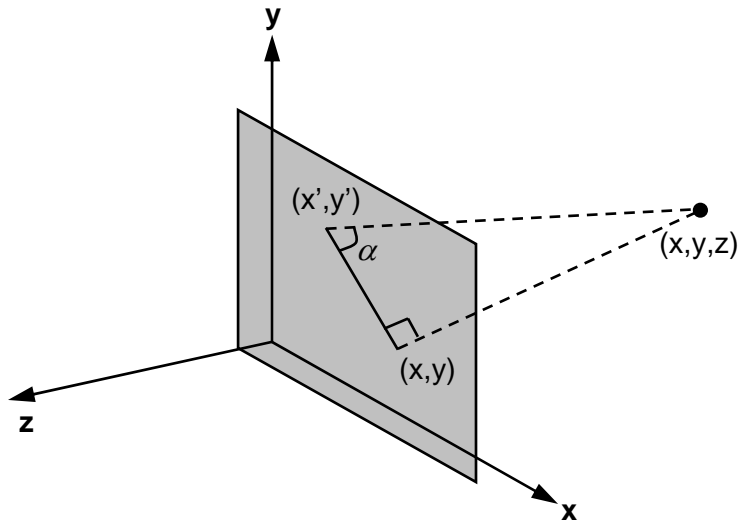


Fig. 3.7 Conversion of 3D coordinate point to the view plane for an oblique projection

Fig. 3.7 shows the projection of a point (x, y, z) to the point (x', y') onto the view plane. Angle *alpha* is defined as the angle between the oblique projection line

from (x, y, z) to (x', y') and the line on the view plane from (x, y) to (x', y') . Two commonly used values for α is 45° and 63.4° .

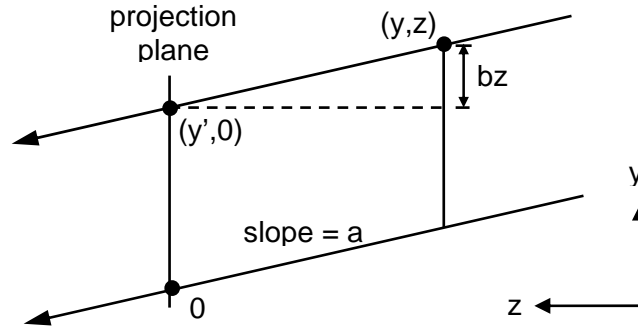


Fig. 3.8 Oblique projection

From Fig. 3.8, oblique projection can be implemented mathematically as follow:

$$\begin{bmatrix} x' \\ y' \\ 1 \end{bmatrix} = \begin{bmatrix} x - az \\ y - bz \\ 1 \end{bmatrix} = \begin{bmatrix} 1 & 0 & -a & 0 \\ 0 & 1 & -b & 0 \\ 0 & 0 & 1 & 0 \\ 0 & 0 & 0 & 1 \end{bmatrix} \begin{bmatrix} x \\ y \\ z \\ 1 \end{bmatrix} \quad (3.2)$$

where $a = \text{slope or } \tan \alpha$;

$b = \text{sine } \alpha$;

$\alpha = \text{the angle between the oblique projection and the line on the view plane}$

3.2.2 Perspective Projections

Perspective projection diminishes the objects being projected with distance, until they all converge at a “vanishing point” at infinity. The center of projection (PRP) is placed at a finite distance from the view plane; therefore, the projectors are no longer parallel. By placing the camera near the view plane, as shown in Figure 3.9, projectors from the PRP to the edges of the projection window define a pyramidal view volume.

The projectors from the center of projection to line AB form a much shorter line A'B' in the view plane. The decreasing distance between the two projectors indicate that the viewing surface becomes nearer to the center of projection.

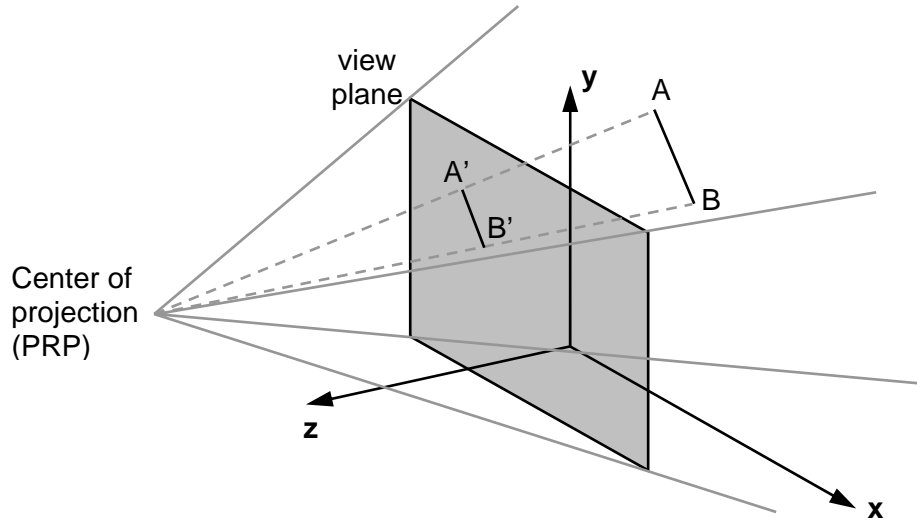


Fig. 3.9 Pyramidal view volume for a perspective projection

Perspective projection can be easily formulated by similar triangles as shown in

Fig. (3.10)

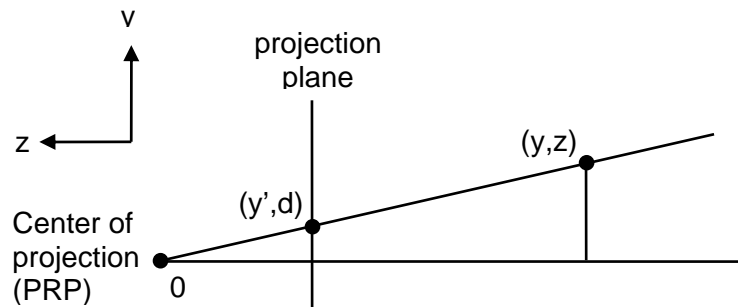


Fig. 3.10 Perspective projection

Similar triangles:

$$\frac{y'}{d} = \frac{y}{z}$$

$$y' = \frac{dy}{z}$$

, assumed that the location of point d and z in Fig. 3.10 are far from the center of projection $\left(\frac{d}{z} \approx 1\right)$ and the matrix expression is

$$\begin{bmatrix} x' \\ y' \\ 1 \end{bmatrix} = \begin{bmatrix} \frac{dx}{z} \\ \frac{dy}{z} \\ \frac{z}{1} \end{bmatrix} \approx \begin{bmatrix} x \\ y \\ \frac{z}{d} \end{bmatrix} = \begin{bmatrix} 1 & 0 & 0 & 0 \\ 0 & 1 & 0 & 0 \\ 0 & 0 & 1/d & 0 \end{bmatrix} \begin{bmatrix} x \\ y \\ z \\ 1 \end{bmatrix} \quad (3.3)$$

Perspective projections are typically separated into three classes: *one-point*, *two-point*, and *three-point* projections. Each class differs in the orientation of the view plane and the number of vanishing points the unit cube has.

In a *one-point* perspective as shown in Fig. 3.11, lines of a three-dimensional object along a major axis converge to a single vanishing point while lines parallel to the other axes remain horizontal or vertical in the view plane refer to Hill (1990). In this projection, the view plane is positioned in front of the cube and parallel to the x - and y -plane.

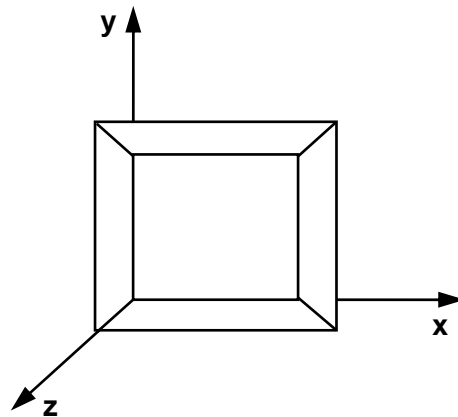


Fig. 3.11 One-point perspective projection

A *two-point* perspective as shown in Fig 3.12 projects an object to the view plane such that lines parallel to two of the major axes converge into two separate vanishing points. Fig. 3.12 presents lines parallel to the x-axis converge to vanishing point VP1 while lines parallel to the z-axis converge to vanishing point VP2

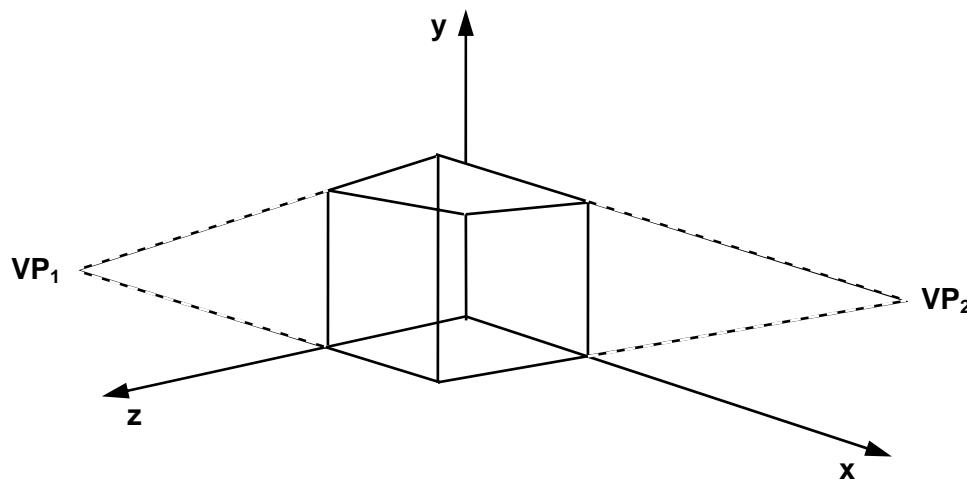


Fig. 3.12 Two-point perspective projection

Finally, a *three-point* perspective has three vanishing points (Hill (1990)). In this case, the view plane is not parallel to any of the major axes.

CHAPTER IV

FINITE ELEMENT FORMULATION AND PROGRAM IMPLEMENTATION

4.1 Coordinate Systems and Transformation Matrix

In finite element analysis, a properly defined coordinate system is essential in the process of implementing the computer program. All parameters in one equation need to be converted to the same coordinate system in every computational steps. In addition, to develop a convenient and user-friendly analysis program, the loads data may be referred to either global or local coordinate depending on the information that user already have. Furthermore, to represent the result, e.g., displacement, rotation, and internal force, from the computation, the appropriate coordinate is preferred to make the result simple for further verification.

4.1.1 The Global Coordinate System

The global-global coordinate system is a typically cartesian coordinate system used for describing the geometry for the complete structure. Global coordinates are used as a reference system for the formulation of stiffness and applied force matrices as well as graphical representation of the mathematical model. Using the right hand screw rule to define the sign of moments and set up the positive direction of x, y, z axes, the global coordinate system is shown in Fig. 4.1.

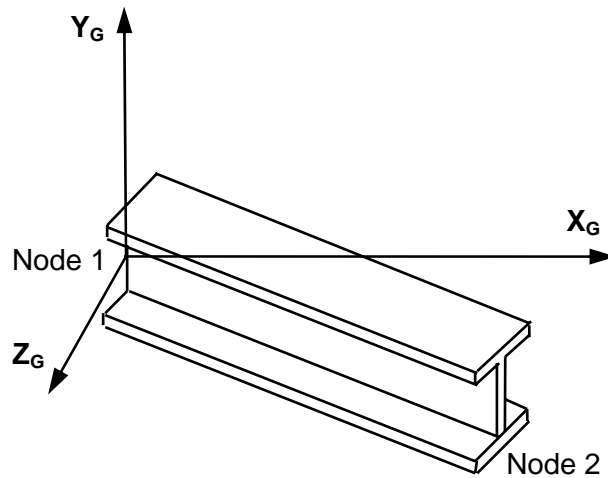


Fig. 4.1 The global coordinate system

4.1.2 The Local Coordinate System

An element is typically defined in its local coordinate system initially. The local coordinate system is independent of the world coordinate system in which the member is placed with other members to form a whole structure. When an element does not have an orientation, its local coordinate system coincide with the structure global coordinate system, each element stiffness must be transformed to the global axes so that member with different orientations can be summed to make a further computation. A typical element local coordinate system for a general steel member is shown in Fig. 4.2.

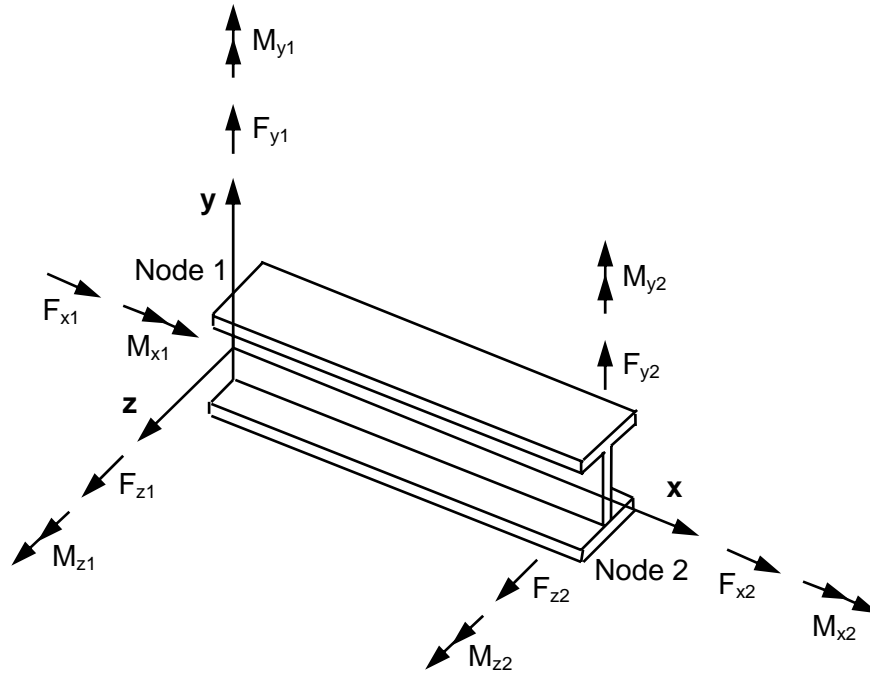


Fig. 4.2 The local coordinate system

4.1.3 The Transformation Matrix[2]

Local coordinate system can be related to global coordinate system by a transformation matrix. The transformation matrix for three dimensional elements can be expressed as

$$[T] = \begin{bmatrix} \lambda_{3 \times 3} & 0 & 0 & 0 \\ 0 & \lambda_{3 \times 3} & 0 & 0 \\ 0 & 0 & \lambda_{3 \times 3} & 0 \\ 0 & 0 & 0 & \lambda_{3 \times 3} \end{bmatrix} \quad (4.1)$$

where:

$$\lambda = \begin{bmatrix} C_{x\hat{x}} & C_{y\hat{x}} & C_{z\hat{x}} \\ C_{x\hat{y}} & C_{y\hat{y}} & C_{z\hat{y}} \\ C_{x\hat{z}} & C_{y\hat{z}} & C_{z\hat{z}} \end{bmatrix} \quad (4.2)$$

The parameters $C_{x\hat{x}}, C_{y\hat{x}}, \dots$ are the direction cosines of angle between global and local coordinate system as shown in Fig. 4.3. For example, direction cosines of $C_{x\hat{x}}, C_{y\hat{x}}$ and $C_{z\hat{x}}$ are $\cos \theta_{x\hat{x}}, \cos \theta_{y\hat{x}}$, and $\cos \theta_{z\hat{x}}$, respectively. This can be expressed as:

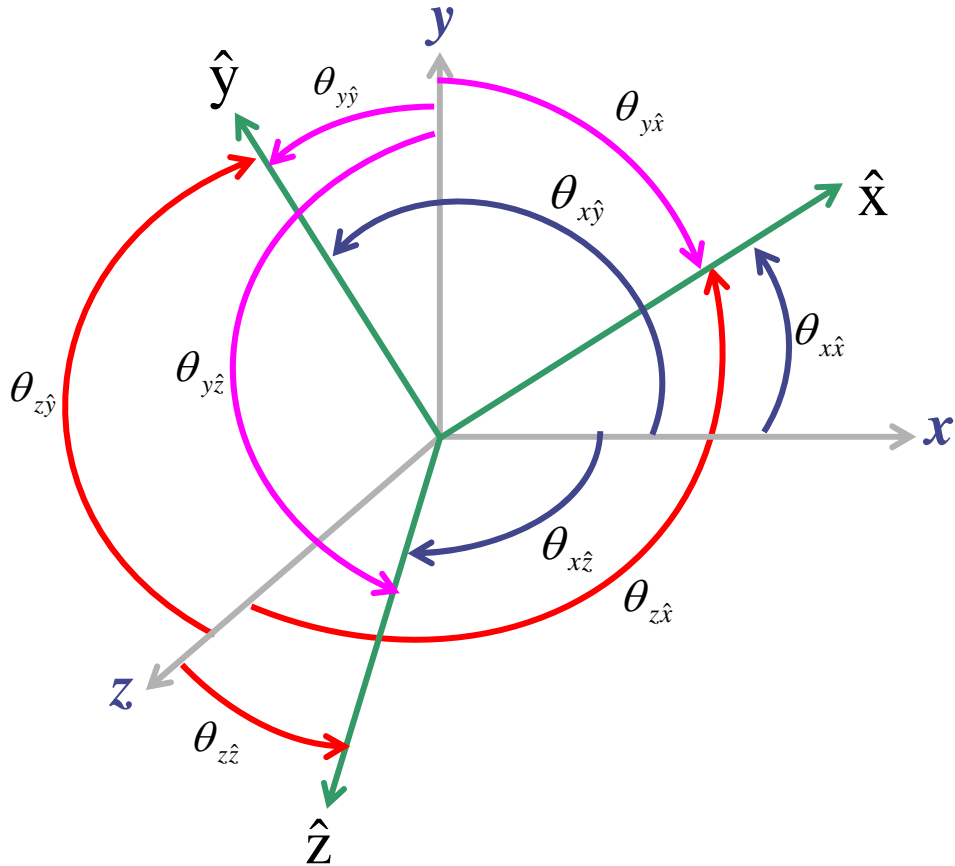


Fig. 4.3 Definition of angles between global and local coordinate system

$$\hat{u}_{\hat{x}} = \cos_{x\hat{x}} \hat{i} + \cos_{y\hat{x}} \hat{j} + \cos_{z\hat{x}} \hat{k} \quad (4.3)$$

The three transformation angles related to x-axis can be written as

$$\cos_{x\hat{x}} = \frac{x_j - x_i}{L} = l$$

$$\cos_{y\hat{x}} = \frac{y_j - y_i}{L} = m \quad (4.4)$$

$$\cos_{\hat{x}} = \frac{z_j - z_i}{L} = n$$

where $x_i, y_i, z_i, x_j, y_j,$ and z_j are the i^{th} and j^{th} coordinated of a vector on the x, y, and z axes. The three angles related to \hat{y} -axis and \hat{z} -axis can be formulated using the method of successive rotations as illustrate in Fig. 4.4.

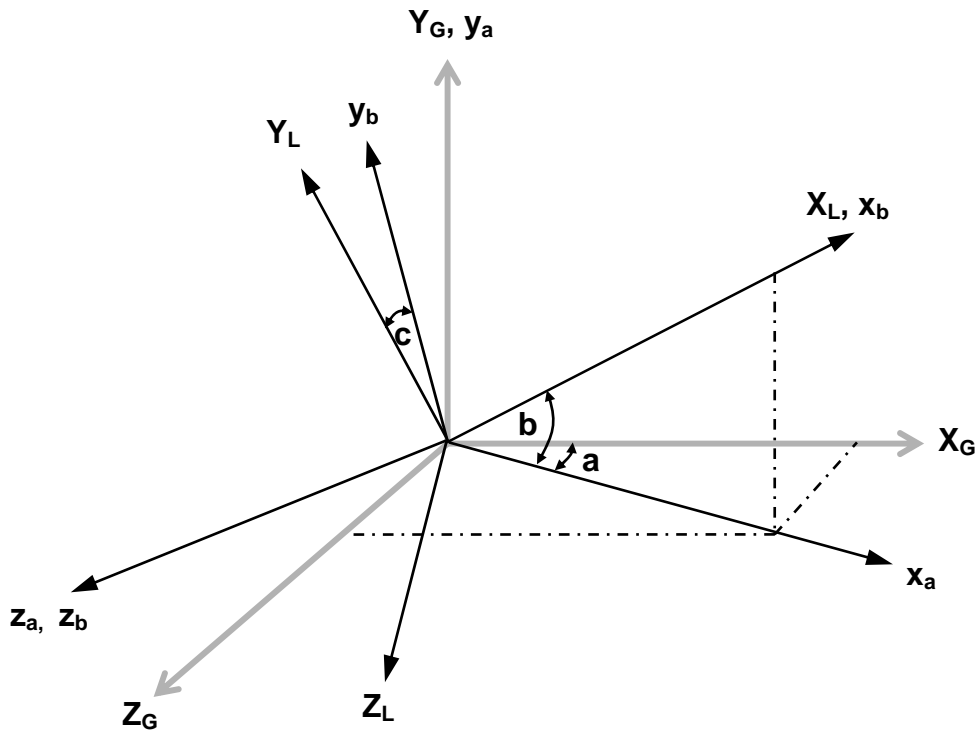


Fig. 4.4 Successive rotations method[2]

In order to rotate the coordinates from the global system to the local system, first consider a rotation about the Y_G axis by an angle a . The resulting coordinate system may be designated the a system. The necessary rotation matrix R_a for performed this rotation are expressed in term of a as follow:

$$R_a = \begin{bmatrix} \cos a & 0 & \sin a \\ 0 & 1 & 0 \\ -\sin a & 0 & \cos a \end{bmatrix} \quad (4.5)$$

A second rotation may now be accomplished through the angle b and about the new z_a axis. The resulting axes are now designated the b system, the rotation matrix is called R_b , and the general set of value in terms of the new coordinate is given by:

$$R_b = \begin{bmatrix} \cos b & \sin b & 0 \\ -\sin b & \cos b & 0 \\ 0 & 0 & 1 \end{bmatrix} \quad (4.6)$$

The final rotation necessary to ensure that the structure axis coincides with the member axis is a rotation about the x_b axes through the angle c . This third rotation of axes is necessary only if the y_b and z_b axes do not coincide with the local coordinate system. In general, the axes may not be the same; however, in particular cases, such as members whose cross-section is symmetrical about more than one axis, a third rotation may not be necessary. Designating the final rotation matrix R_c may now be found by:

$$R_c = \begin{bmatrix} 1 & 0 & 0 \\ 0 & \cos c & \sin c \\ 0 & -\sin c & \cos c \end{bmatrix} \quad (4.7)$$

Finally, the transformation matrix can be formulated by:

$$\lambda = \begin{bmatrix} C_{x\hat{x}} & C_{y\hat{x}} & C_{z\hat{x}} \\ C_{x\hat{y}} & C_{y\hat{y}} & C_{z\hat{y}} \\ C_{x\hat{z}} & C_{y\hat{z}} & C_{z\hat{z}} \end{bmatrix} = R_c R_b R_a \quad (4.8)$$

$$\lambda = \begin{bmatrix} \cos a \cos b & \sin b & \cos b \sin a \\ -\cos a \cos c \sin b - \sin a \sin c & \cos b \cos c & -\cos c \sin a \sin b + \cos a \sin c \\ -\cos c \sin a + \cos a \sin b \sin c & -\cos b \sin c & \cos a \cos c + \sin a \sin b \sin c \end{bmatrix}$$

Therefore, the element stiffness matrix in the local coordinate system can be transformed into global coordinate system by

$$[k] = [T]^T [k^e] [T] \quad (4.9)$$

In conclusion, Equations 4.8 and 4.9 are the final formulas of the transformation matrix for three dimensional elements which is used in developing the element algorithm in the later section.

4.2 Element Stiffness Formulation

To derive the local stiffness of the three dimensional beam element, the element stiffness matrix for the two dimensional one (Fig. 4.5) is recalled as follow,

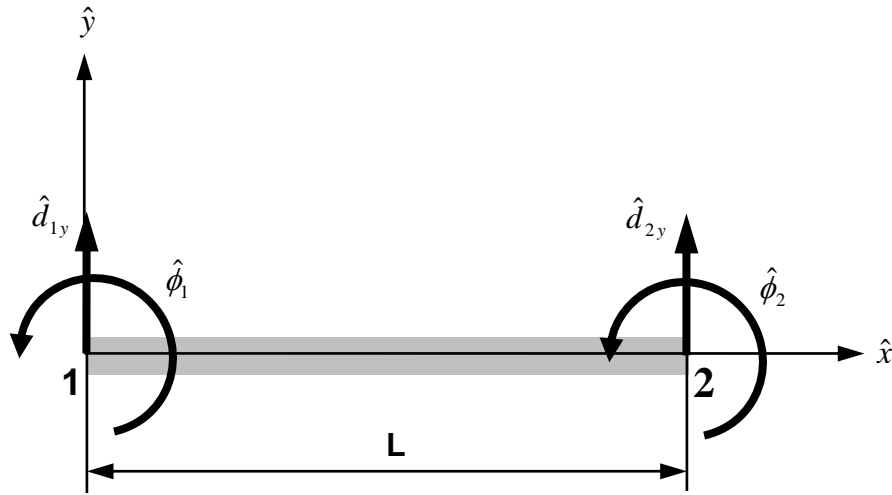


Fig. 4.5 Two dimensional beam member

$$\begin{Bmatrix} \hat{f}_{1,y} \\ \hat{m}_1 \\ \hat{f}_{2,y} \\ \hat{m}_2 \end{Bmatrix} = \frac{EI}{L^3} \begin{bmatrix} 12 & 6L & -12 & 6L \\ 6L & 4L^2 & -6L & 2L^2 \\ -12 & -6L & 12 & -6L \\ 6L & 2L^2 & -6L & 4L^2 \end{bmatrix} \begin{Bmatrix} \hat{d}_{1,y} \\ \hat{\phi}_1 \\ \hat{d}_{2,y} \\ \hat{\phi}_2 \end{Bmatrix} \quad (4.10)$$

Fig. 4.6 shows bending in two planes for the three dimensional beam member, stiffness matrix for bending in each $\hat{x}-\hat{y}$ and $\hat{x}-\hat{z}$ plane can be derived same as Equation 4.10 which are

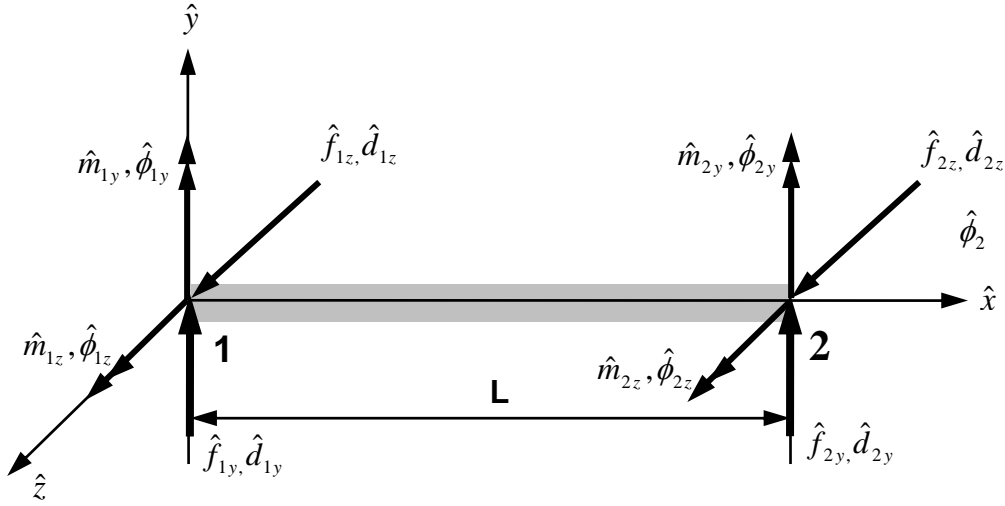


Fig. 4.6 Bending in two planes

$$\text{Bending in } \hat{x}-\hat{y} \text{ plane, } \left[\hat{k}_z \right] = \frac{EI_z}{L^3} \begin{bmatrix} 12 & 6L & -12 & 6L \\ 6L & 4L^2 & -6L & 2L^2 \\ -12 & -6L & 12 & -6L \\ 6L & 2L^2 & -6L & 4L^2 \end{bmatrix} \quad (4.11)$$

$$\text{Bending in } \hat{x}-\hat{z} \text{ plane, } \left[\hat{k}_y \right] = \frac{EI_y}{L^3} \begin{bmatrix} 12 & 6L & -12 & 6L \\ 6L & 4L^2 & -6L & 2L^2 \\ -12 & -6L & 12 & -6L \\ 6L & 2L^2 & -6L & 4L^2 \end{bmatrix} \quad (4.12)$$

To formulate element stiffness for 12 DOF three dimensional beam element; axial stiffness, torsional stiffness, and two bending stiffness are combined together. The stiffness of axial forces and torsions are as follow:

$$\text{Axial equilibrium equation, } \begin{Bmatrix} \hat{f}_{1x} \\ \hat{f}_{2x} \end{Bmatrix} = \frac{AE}{L} \begin{bmatrix} 1 & -1 \\ -1 & 1 \end{bmatrix} \begin{Bmatrix} \hat{d}_{1x} \\ \hat{d}_{2x} \end{Bmatrix} \quad (4.13)$$

$$\text{Torsional equilibrium equation, } \begin{Bmatrix} \hat{m}_{1x} \\ \hat{m}_{2x} \end{Bmatrix} = \frac{GJ}{L} \begin{bmatrix} 1 & -1 \\ -1 & 1 \end{bmatrix} \begin{Bmatrix} \hat{\phi}_{1x} \\ \hat{\phi}_{2x} \end{Bmatrix} \quad (4.14)$$

The complete element stiffness matrix for three dimension beam member can be obtained by adding Equations 4.11, 4.12, 4.13, and 4.14 as follows:

$$[\hat{k}^e]_{12 \times 12} = \begin{bmatrix} \bar{k}_{11} & \bar{k}_{12} \\ \bar{k}_{21} & \bar{k}_{22} \end{bmatrix} \quad (4.15)$$

$$[\bar{k}_{11}] = \begin{bmatrix} \frac{AE}{L} & 0 & 0 & 0 & 0 & 0 \\ 0 & \frac{12EI_z}{L^3} & 0 & 0 & 0 & \frac{6EI_z}{L^2} \\ 0 & 0 & \frac{12EI_y}{L^3} & 0 & -\frac{6EI_y}{L^2} & 0 \\ 0 & 0 & 0 & \frac{GJ}{L} & 0 & 0 \\ 0 & 0 & -\frac{6EI_y}{L^2} & 0 & \frac{4EI_y}{L} & 0 \\ 0 & \frac{6EI_z}{L^2} & 0 & 0 & 0 & \frac{4EI_z}{L} \end{bmatrix} \quad (4.16)$$

$$[\bar{k}_{12}] = \begin{bmatrix} -\frac{AE}{L} & 0 & 0 & 0 & 0 & 0 \\ 0 & -\frac{12EI_z}{L^3} & 0 & 0 & 0 & \frac{6EI_z}{L^2} \\ 0 & 0 & -\frac{12EI_y}{L^3} & 0 & -\frac{6EI_y}{L^2} & 0 \\ 0 & 0 & 0 & -\frac{GJ}{L} & 0 & 0 \\ 0 & 0 & \frac{6EI_y}{L^2} & 0 & \frac{2EI_y}{L} & 0 \\ 0 & -\frac{6EI_z}{L^2} & 0 & 0 & 0 & \frac{2EI_z}{L} \end{bmatrix} \quad (4.17)$$

$$[\bar{k}_{21}] = \begin{bmatrix} -\frac{AE}{L} & 0 & 0 & 0 & 0 & 0 \\ 0 & -\frac{12EI_z}{L^3} & 0 & 0 & 0 & \frac{6EI_z}{L^2} \\ 0 & 0 & -\frac{12EI_y}{L^3} & 0 & \frac{6EI_y}{L^2} & 0 \\ 0 & 0 & 0 & -\frac{GJ}{L} & 0 & 0 \\ 0 & 0 & -\frac{6EI_y}{L^2} & 0 & \frac{2EI_y}{L} & 0 \\ 0 & \frac{6EI_z}{L^2} & 0 & 0 & 0 & \frac{2EI_z}{L} \end{bmatrix} \quad (4.18)$$

$$[\bar{k}_{22}] = \begin{bmatrix} \frac{AE}{L} & 0 & 0 & 0 & 0 & 0 \\ 0 & \frac{12EI_z}{L^3} & 0 & 0 & 0 & -\frac{6EI_z}{L^2} \\ 0 & 0 & \frac{12EI_y}{L^3} & 0 & \frac{6EI_y}{L^2} & 0 \\ 0 & 0 & 0 & \frac{GJ}{L} & 0 & 0 \\ 0 & 0 & \frac{6EI_y}{L^2} & 0 & \frac{4EI_y}{L} & 0 \\ 0 & -\frac{6EI_z}{L^2} & 0 & 0 & 0 & \frac{4EI_z}{L} \end{bmatrix} \quad (4.19)$$

Because the total 12 DOFs are not fully independent, the stiffness matrix can be reduced to the equivalent six active forces and moments stiffness as follow,

$$[\hat{k}^e]_{6 \times 6} [u] = [P]$$

$$\begin{bmatrix} \frac{EA}{L} & 0 & 0 & 0 & 0 & 0 \\ 0 & \frac{4EI_y}{L} & 0 & 0 & \frac{2EI_y}{L} & 0 \\ 0 & 0 & \frac{4EI_z}{L} & 0 & 0 & \frac{2EI_z}{L} \\ 0 & 0 & 0 & \frac{GJ}{L} & 0 & 0 \\ 0 & \frac{2EI_y}{L} & 0 & 0 & \frac{4EI_y}{L} & 0 \\ 0 & 0 & \frac{2EI_z}{L} & 0 & 0 & \frac{4EI_z}{L} \end{bmatrix} \begin{bmatrix} d_x \\ \phi_{y1} \\ \phi_{z1} \\ \phi_x \\ \phi_{y2} \\ \phi_{z2} \end{bmatrix} = \begin{bmatrix} F_x \\ M_{y1} \\ M_{z1} \\ M_x \\ M_{y2} \\ M_{z2} \end{bmatrix} \quad (4.20)$$

This 6 DOFs stiffness matrix can be related to total twelve forces and moments stiffness matrix in Equations 4.17-4.21 by the transformation matrix $[T_k]$ which is

$$[T_k] = \begin{bmatrix} -1 & 0 & 0 & 0 & 0 & 0 \\ 0 & 0 & 1/L & 0 & 0 & 1/L \\ 0 & -1/L & 0 & 0 & -1/L & 0 \\ 0 & 0 & 0 & -1 & 0 & 0 \\ 0 & 1 & 0 & 0 & 0 & 0 \\ 0 & 0 & 1 & 0 & 0 & 0 \\ 1 & 0 & 0 & 0 & 0 & 0 \\ 0 & 0 & -1/L & 0 & 0 & -1/L \\ 0 & 1/L & 0 & 0 & 1/L & 0 \\ 0 & 0 & 0 & 1 & 0 & 0 \\ 0 & 0 & 0 & 0 & 1 & 0 \\ 0 & 0 & 0 & 0 & 0 & 1 \end{bmatrix} \quad (4.21)$$

$$[k^e]_{12 \times 12} = [T_k] [k^e]_{6 \times 6} [T]^T \quad (4.22)$$

The reduced stiffness formula in Equation 4.20 allows to simply formulate the modified stiffness matrix for hybrid element by considering semi-rigid connection or yielding effect which will explain in detail in Section 4.4. This stiffness and their transformation, Equation 4.21, will be employed through this study.

4.3 Tangent and Geometric Stiffness Formulation

In non-linear analysis, the geometric stiffness matrix $[k_G]$ is added to the linear stiffness matrix $[k_L]$ to include the instability effect due to initial stress of the element. The combining form of stiffness matrix, so called tangent stiffness matrix $[k_T]$, accounting non-linear effects can be expressed as

$$[k_T] = [k_L] + [k_G] + [k_o] \quad (4.23)$$

in which $[k_o]$ is the large displacement matrix.

The large displacement matrix caters the effect of changing in geometry which can be automatically evaluated in the computation by continuous updating the structure geometry in each iteration of non-linear analysis. The linear stiffness matrix has been explained previously in Section 4.2. The geometric stiffness matrix can be expressed as the work done by the initial stresses or forces and the second-order displacements as

$$[k_G] = \frac{P}{2} \left[\int_0^L \left(\frac{\partial v}{\partial x} \right)^2 + \left(\frac{\partial w}{\partial x} \right)^2 dx \right] \quad (4.24)$$

where:

$$\begin{aligned} v &= \left(1 - \frac{x}{L} \right) v_1 + \frac{x}{L} v_2 \\ w &= \left(1 - \frac{x}{L} \right) w_1 + \frac{x}{L} w_2 \end{aligned} \quad (4.25)$$

For displacement in y-axis, Equation 4.24 can be expressed as

$$N_{ij} = \frac{P}{2} \int_L \left(\frac{\partial v}{\partial x} \right)^2 dx \quad (4.26)$$

where N_{ij} is the component of $[N]$ accounting for work done by the initial forces and the nodal displacements in y-axis. Substituting Equation 4.25 in to Equation 4.26, one obtains

$$\begin{aligned} N_{ij} &= P/L \quad \text{for } i = j, \\ N_{ij} &= -P/L \quad \text{for } i \neq j \end{aligned} \tag{4.27}$$

The effect of displacement in z-axis can be obtained by the same procedure. Finally, the geometry stiffness matrix is obtained as follow,

$$[N] = \begin{bmatrix} 0 & 0 & 0 & 0 & 0 & 0 & 0 & 0 & 0 & 0 & 0 \\ 0 & P/L & 0 & 0 & 0 & 0 & -P/L & 0 & 0 & 0 & 0 \\ 0 & 0 & P/L & 0 & 0 & 0 & 0 & -P/L & 0 & 0 & 0 \\ 0 & 0 & 0 & 0 & 0 & 0 & 0 & 0 & 0 & 0 & 0 \\ 0 & 0 & 0 & 0 & 0 & 0 & 0 & 0 & 0 & 0 & 0 \\ 0 & 0 & 0 & 0 & 0 & 0 & 0 & 0 & 0 & 0 & 0 \\ 0 & 0 & 0 & 0 & 0 & 0 & 0 & 0 & 0 & 0 & 0 \\ 0 & -P/L & 0 & 0 & 0 & 0 & P/L & 0 & 0 & 0 & 0 \\ 0 & 0 & -P/L & 0 & 0 & 0 & 0 & P/L & 0 & 0 & 0 \\ 0 & 0 & 0 & 0 & 0 & 0 & 0 & 0 & 0 & 0 & 0 \\ 0 & 0 & 0 & 0 & 0 & 0 & 0 & 0 & 0 & 0 & 0 \\ 0 & 0 & 0 & 0 & 0 & 0 & 0 & 0 & 0 & 0 & 0 \end{bmatrix} \tag{4.28}$$

Finally, the tangent stiffness matrix can be express as,

$$K_T = \sum_{j=1}^{NELE} k_T = \sum_{j=1}^{NELE} [T]^T ([k]_{12 \times 12} + [N])[T] \tag{4.29}$$

which can be rewritten in term of six element forces and moments as

$$K_T = \sum_{j=1}^{NELE} k_T = \sum_{j=1}^{NELE} [T]^T ([T_k] [k]_{6 \times 6} [T_k]^T + [N])[T] \tag{4.30}$$

4.4 Modified Element Stiffness Accounting for the Effects of Joint Flexibility and Material Yielding

4.4.1 Hybrid Element with Connection Spring

To include the effect of semi-rigid connection, a pseudo-rotation-spring or the connection spring element is used to model the connection element in this present study. This spring element is connected to the two ends of beam-column member forming a hybrid element as shown in Fig. 4.7. The internal moments and rotations at a connection spring at deformed state are illustrated in Fig. 4.8 in which the rotation of a connection is defined as the relative angle between the two sides of the connection (i.e. $\phi_c = \theta_c - \theta_b$).

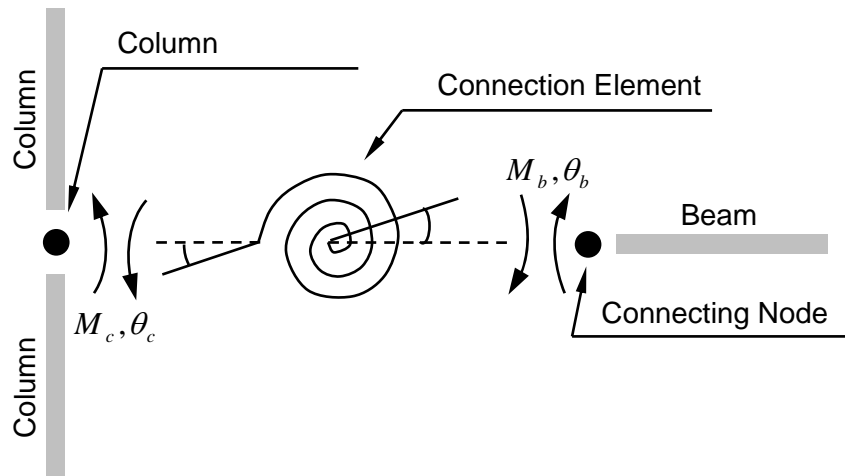


Fig. 4.7 Column spring element[1]

In Fig. 4.8, the flexural element stiffness for the inner part of hybrid element can be expressed as

$$\begin{Bmatrix} \Delta M_{bi} \\ \Delta M_{bj} \end{Bmatrix} = \begin{bmatrix} K_{ii} & K_{ij} \\ K_{ji} & K_{jj} \end{bmatrix} \begin{Bmatrix} \Delta \theta_{bi} \\ \Delta \theta_{bj} \end{Bmatrix} \quad (4.31)$$

in which subscript i and j are referred to end node i and j, and K_{ij} is the element flexural stiffness about z-axes of the beam-column element.

Considering the connection spring at two end of hybrid element, the stiffness for each part can be formulated, for node i,

$$\Delta M_{ci} = S_{ci}(\Delta \theta_{ci} - \Delta \theta_{bi}) = S_{ci}\Delta \theta_{ci} - S_{ci}\Delta \theta_{bi} \quad (4.32)$$

$$\Delta M_{bi} = S_{ci}(\Delta \theta_{bi} - \Delta \theta_{ci}) = -S_{ci}\Delta \theta_{ci} + S_{ci}\Delta \theta_{bi} \quad (4.33)$$

Equations 4.32 and 4.33 can be rewritten in the matrix form as follow

$$\begin{Bmatrix} \Delta M_{ci} \\ \Delta M_{bi} \end{Bmatrix} = \begin{bmatrix} S_{ci} & -S_{ci} \\ -S_{ci} & S_{ci} \end{bmatrix} \begin{Bmatrix} \Delta \theta_{ci} \\ \Delta \theta_{bi} \end{Bmatrix} \quad (4.34)$$

in which S_{ci} is the connection stiffness at node i, and for node j,

$$\Delta M_{bj} = S_{cj}(\Delta \theta_{bj} - \Delta \theta_{cj}) = S_{cj}\Delta \theta_{bj} - S_{cj}\Delta \theta_{cj} \quad (4.35)$$

$$\Delta M_{cj} = S_{cj}(\Delta \theta_{cj} - \Delta \theta_{bj}) = -S_{cj}\Delta \theta_{bj} + S_{cj}\Delta \theta_{cj} \quad (4.36)$$

Equations 4.35 and 4.36 can be rewritten in the matrix form as follow:

$$\begin{Bmatrix} \Delta M_{bj} \\ \Delta M_{cj} \end{Bmatrix} = \begin{bmatrix} S_{cj} & -S_{cj} \\ -S_{cj} & S_{cj} \end{bmatrix} \begin{Bmatrix} \Delta \theta_{bj} \\ \Delta \theta_{cj} \end{Bmatrix} \quad (4.37)$$

, in which S_{cj} is the connection stiffness at node j.

Combining all three parts of hybrid element stiffness matrix, Equations 4.31, 4.34, 4.37 are assembled together, which results:

$$\begin{Bmatrix} \Delta M_{ci} \\ \Delta M_{bi} \\ \Delta M_{bj} \\ \Delta M_{cj} \end{Bmatrix} = \begin{bmatrix} S_{ci} & -S_{ci} & 0 & 0 \\ -S_{ci} & S_{ci} + K_{ii} & K_{ij} & 0 \\ 0 & K_{ji} & S_{cj} + K_{jj} & -S_{cj} \\ 0 & 0 & -S_{cj} & S_{cj} \end{bmatrix} \begin{Bmatrix} \Delta \theta_{ci} \\ \Delta \theta_{bi} \\ \Delta \theta_{bj} \\ \Delta \theta_{cj} \end{Bmatrix} \quad (4.38)$$

To eliminate the internal degrees of freedom, assume that loads are applied only at global nodes such that ΔM_{bi} and ΔM_{bj} are equal to zero. The matrix can be condensed as follow

$$\begin{Bmatrix} 0 \\ 0 \end{Bmatrix} = \begin{bmatrix} -S_{ci} & 0 \\ 0 & -S_{cj} \end{bmatrix} \begin{Bmatrix} \Delta \theta_{ci} \\ \Delta \theta_{cj} \end{Bmatrix} + \begin{bmatrix} S_{ci} + K_{ii} & K_{ij} \\ K_{ji} & S_{cj} + K_{jj} \end{bmatrix} \begin{Bmatrix} \Delta \theta_{bi} \\ \Delta \theta_{bj} \end{Bmatrix}$$

$$\begin{bmatrix} S_{ci} + K_{ii} & K_{ij} \\ K_{ji} & S_{cj} + K_{jj} \end{bmatrix} \begin{Bmatrix} \Delta \theta_{bi} \\ \Delta \theta_{bj} \end{Bmatrix} = \begin{bmatrix} S_{ci} & 0 \\ 0 & S_{cj} \end{bmatrix} \begin{Bmatrix} \Delta \theta_{ci} \\ \Delta \theta_{cj} \end{Bmatrix}$$

$$\begin{Bmatrix} \Delta \theta_{bi} \\ \Delta \theta_{bj} \end{Bmatrix} = \begin{bmatrix} S_{ci} + K_{ii} & K_{ij} \\ K_{ji} & S_{cj} + K_{jj} \end{bmatrix}^{-1} \begin{bmatrix} S_{ci} & 0 \\ 0 & S_{cj} \end{bmatrix} \begin{Bmatrix} \Delta \theta_{ci} \\ \Delta \theta_{cj} \end{Bmatrix} \quad (4.39)$$

Substituting Equation 4.39 into 4.38, thus we obtain

$$\begin{Bmatrix} \Delta M_{ci} \\ \Delta M_{cj} \end{Bmatrix} = \begin{bmatrix} S_{ci} & 0 \\ 0 & S_{cj} \end{bmatrix} \begin{Bmatrix} \Delta \theta_{ci} \\ \Delta \theta_{cj} \end{Bmatrix} + \begin{bmatrix} -S_{ci} & 0 \\ 0 & -S_{cj} \end{bmatrix} \begin{Bmatrix} \Delta \theta_{bi} \\ \Delta \theta_{bj} \end{Bmatrix}$$

$$\begin{Bmatrix} \Delta M_{ci} \\ \Delta M_{cj} \end{Bmatrix} = \begin{bmatrix} S_{ci} & 0 \\ 0 & S_{cj} \end{bmatrix} \begin{Bmatrix} \Delta \theta_{ci} \\ \Delta \theta_{cj} \end{Bmatrix} + \begin{bmatrix} -S_{ci} & 0 \\ 0 & -S_{cj} \end{bmatrix} \left(\begin{bmatrix} S_{ci} + K_{ii} & K_{ij} \\ K_{ji} & S_{cj} + K_{jj} \end{bmatrix}^{-1} \begin{bmatrix} S_{ci} & 0 \\ 0 & S_{cj} \end{bmatrix} \begin{Bmatrix} \Delta \theta_{ci} \\ \Delta \theta_{cj} \end{Bmatrix} \right)$$

$$\begin{Bmatrix} \Delta M_{ci} \\ \Delta M_{cj} \end{Bmatrix} = \left(\begin{bmatrix} S_{ci} & 0 \\ 0 & S_{cj} \end{bmatrix} - \frac{\begin{bmatrix} S_{ci} & 0 \\ 0 & S_{cj} \end{bmatrix} \begin{bmatrix} S_{cj} + K_{jj} & -K_{ij} \\ -K_{ji} & S_{ci} + K_{ii} \end{bmatrix} \begin{bmatrix} S_{ci} & 0 \\ 0 & S_{cj} \end{bmatrix}}{(S_{ci} + K_{ii})(S_{cj} + K_{jj}) - K_{ij}K_{ji}} \right) \begin{Bmatrix} \Delta \theta_{ci} \\ \Delta \theta_{cj} \end{Bmatrix} \quad (4.40)$$

Equation 4.40 is the modified flexural stiffness for beam-column element including the effect of semi-rigid connection at both ends. Alternately, to formulate the modified flexural stiffness for beam-column element that has connection at one end, Equation 4.38 can be used by adding only the stiffness of existing connection. Then repeat all the procedure of static condensation. The formula can be expressed as follow, for semi-rigid at node i:

$$\begin{Bmatrix} \Delta M_{ci} \\ \Delta M_{bi} \\ \Delta M_j \end{Bmatrix} = \begin{bmatrix} S_{ci} & -S_{ci} & 0 \\ -S_{ci} & S_{ci} + K_{ii} & K_{ij} \\ 0 & K_{ji} & K_{jj} \end{bmatrix} \begin{Bmatrix} \Delta \theta_{ci} \\ \Delta \theta_{bi} \\ \Delta \theta_j \end{Bmatrix} \quad (4.41)$$

Set ΔM_{bi} equal to zero, we have

$$\begin{aligned} 0 &= \begin{bmatrix} -S_{ci} & K_{ij} \end{bmatrix} \begin{Bmatrix} \Delta \theta_{ci} \\ \Delta \theta_j \end{Bmatrix} + (S_{ci} + K_{ii})(\Delta \theta_{bi}) \\ (S_{ci} + K_{ii})(\Delta \theta_{bi}) &= \begin{bmatrix} S_{ci} & -K_{ij} \end{bmatrix} \begin{Bmatrix} \Delta \theta_{ci} \\ \Delta \theta_j \end{Bmatrix} \\ (\Delta \theta_{bi}) &= \frac{\begin{bmatrix} S_{ci} & -K_{ij} \end{bmatrix} \begin{Bmatrix} \Delta \theta_{ci} \\ \Delta \theta_j \end{Bmatrix}}{(S_{ci} + K_{ii})} \end{aligned} \quad (4.42)$$

Substituting Equation 4.42 into 4.41, thus we obtain:

$$\begin{aligned} \begin{Bmatrix} \Delta M_{ci} \\ \Delta M_j \end{Bmatrix} &= \begin{bmatrix} S_{ci} & 0 \\ 0 & K_{jj} \end{bmatrix} \begin{Bmatrix} \Delta \theta_{ci} \\ \Delta \theta_j \end{Bmatrix} + \begin{bmatrix} -S_{ci} \\ K_{ji} \end{bmatrix} \{\Delta \theta_{bi}\} \\ \begin{Bmatrix} \Delta M_{ci} \\ \Delta M_j \end{Bmatrix} &= \left(\begin{bmatrix} S_{ci} & 0 \\ 0 & K_{jj} \end{bmatrix} + \frac{\begin{bmatrix} -S_{ci} \\ K_{ji} \end{bmatrix} \begin{bmatrix} S_{ci} & -K_{ij} \end{bmatrix}}{(S_{ci} + K_{ii})} \right) \begin{Bmatrix} \Delta \theta_{ci} \\ \Delta \theta_j \end{Bmatrix} \end{aligned} \quad (4.43)$$

For eemi-rigid at node j:

$$\begin{Bmatrix} \Delta M_i \\ \Delta M_{bj} \\ \Delta M_{cj} \end{Bmatrix} = \begin{bmatrix} K_{ii} & K_{ij} & 0 \\ K_{ji} & S_{cj} + K_{jj} & -S_{cj} \\ 0 & -S_{cj} & S_{cj} \end{bmatrix} \begin{Bmatrix} \Delta \theta_i \\ \Delta \theta_{bj} \\ \Delta \theta_{cj} \end{Bmatrix} \quad (4.44)$$

Now ΔM_{bj} equal to zero, we have

$$\begin{aligned} 0 &= \begin{bmatrix} K_{ji} & -S_{cj} \end{bmatrix} \begin{Bmatrix} \Delta \theta_i \\ \Delta \theta_{cj} \end{Bmatrix} + (S_{cj} + K_{jj}) (\Delta \theta_{bj}) \\ (S_{cj} + K_{jj}) (\Delta \theta_{bj}) &= \begin{bmatrix} -K_{ji} & S_{cj} \end{bmatrix} \begin{Bmatrix} \Delta \theta_i \\ \Delta \theta_{cj} \end{Bmatrix} \\ (\Delta \theta_{bj}) &= \frac{\begin{bmatrix} -K_{ji} & S_{cj} \end{bmatrix} \begin{Bmatrix} \Delta \theta_i \\ \Delta \theta_{cj} \end{Bmatrix}}{(S_{cj} + K_{jj})} \end{aligned} \quad (4.45)$$

Substituting Equation 4.45 into 4.44, thus we obtain:

$$\begin{aligned} \begin{Bmatrix} \Delta M_i \\ \Delta M_{cj} \end{Bmatrix} &= \begin{bmatrix} K_{ii} & 0 \\ 0 & S_{cj} \end{bmatrix} \begin{Bmatrix} \Delta \theta_i \\ \Delta \theta_{cj} \end{Bmatrix} + \begin{bmatrix} K_{ij} \\ -S_{cj} \end{bmatrix} \{\Delta \theta_{bj}\} \\ \begin{Bmatrix} \Delta M_{ci} \\ \Delta M_j \end{Bmatrix} &= \left(\begin{bmatrix} K_{ii} & 0 \\ 0 & S_{cj} \end{bmatrix} + \frac{\begin{bmatrix} K_{ij} \\ -S_{cj} \end{bmatrix} \begin{bmatrix} -K_{ji} & S_{cj} \end{bmatrix}}{(S_{cj} + K_{jj})} \right) \begin{Bmatrix} \Delta \theta_i \\ \Delta \theta_{cj} \end{Bmatrix} \end{aligned} \quad (4.46)$$

Equations 4.43 and 4.46 are the modified flexural stiffness for beam-column element including the effect of semi-rigid connection at nodes i and j, respectively. Furthermore, to obtain the dependent shear forces of these incremental moments, transformation matrix form Equation 4.21 are employed as follow

$$[T_k] = \begin{bmatrix} -1 & 0 & 0 & 0 & 0 & 0 \\ 0 & 0 & 1/L & 0 & 0 & 1/L \\ 0 & -1/L & 0 & 0 & -1/L & 0 \\ 0 & 0 & 0 & -1 & 0 & 0 \\ 0 & 1 & 0 & 0 & 0 & 0 \\ 0 & 0 & 1 & 0 & 0 & 0 \\ 1 & 0 & 0 & 0 & 0 & 0 \\ 0 & 0 & -1/L & 0 & 0 & -1/L \\ 0 & 1/L & 0 & 0 & 1/L & 0 \\ 0 & 0 & 0 & 1 & 0 & 0 \\ 0 & 0 & 0 & 0 & 1 & 0 \\ 0 & 0 & 0 & 0 & 0 & 1 \end{bmatrix} \quad (4.21)$$

Considering only $M_{z1}, Q_{y1}, M_{z2}, Q_{y2}$, respectively, from Equation 4.21 we obtain

$$[T_k]_{4 \times 2} = \begin{bmatrix} 1 & 0 \\ 1/L & 1/L \\ 0 & 1 \\ -1/L & -1/L \end{bmatrix} \quad (4.47)$$

$$[k^e]_{4 \times 4} = [T_k]_{4 \times 2} [k^e]_{2 \times 2} [T_k]_{4 \times 2}^T \quad (4.48)$$

Equations 4.47 and 4.48 are applied with modified flexural stiffness in Equations 4.40, 4.43, and 4.46 to obtain the both flexural and shear effects of semi-rigid connection. This final term four degrees of freedom modified stiffness will be superimposed on the independent axial and torsional stiffness to form a complete linear stiffness matrix of the element.

4.4.3 Modified Element Stiffness Matrix Accounting for Material yielding

Same as semi-rigid joint effect, material yielding can be included in the analysis by employing hybrid element in Section 4.4.1. The section assemblage method (Section

2.3.3) is used in this study to take into account the yielding effect. Both elastic-plastic hinge and refined-plastic hinge concept based on section assemblage method are applied in the inelastic analysis. In addition, the effect in both y and z axis are considered. Form Equations 4.40, 4.43, and 4.46, modified flexural stiffness can be expressed for plastic hinge at both ends as:

$$\begin{Bmatrix} \Delta M_{pi}^y \\ \Delta M_{pj}^y \end{Bmatrix} = \left(\begin{bmatrix} S_{pi}^y & 0 \\ 0 & S_{pj}^y \end{bmatrix} - \frac{\begin{bmatrix} S_{pi}^y & 0 \\ 0 & S_{pj}^y \end{bmatrix} \begin{bmatrix} S_{pj}^y + K_{jj}^y & -K_{ij}^y \\ -K_{ji}^y & S_{pi}^y + K_{ii}^y \end{bmatrix} \begin{bmatrix} S_{pi}^y & 0 \\ 0 & S_{pj}^y \end{bmatrix}}{(S_{pi}^y + K_{ii}^y)(S_{pj}^y + K_{jj}^y) - K_{ij}^y K_{ji}^y} \right) \begin{Bmatrix} \Delta \theta_{pi}^y \\ \Delta \theta_{pj}^y \end{Bmatrix} \quad (4.49)$$

$$\begin{Bmatrix} \Delta M_{pi}^z \\ \Delta M_{pj}^z \end{Bmatrix} = \left(\begin{bmatrix} S_{pi}^z & 0 \\ 0 & S_{pj}^z \end{bmatrix} - \frac{\begin{bmatrix} S_{pi}^z & 0 \\ 0 & S_{pj}^z \end{bmatrix} \begin{bmatrix} S_{pj}^z + K_{jj}^z & -K_{ij}^z \\ -K_{ji}^z & S_{pi}^z + K_{ii}^z \end{bmatrix} \begin{bmatrix} S_{pi}^z & 0 \\ 0 & S_{pj}^z \end{bmatrix}}{(S_{pi}^z + K_{ii}^z)(S_{pj}^z + K_{jj}^z) - K_{ij}^z K_{ji}^z} \right) \begin{Bmatrix} \Delta \theta_{pi}^z \\ \Delta \theta_{pj}^z \end{Bmatrix} \quad (4.50)$$

Also, for plastic hinge at node i, we have:

$$\begin{Bmatrix} \Delta M_{pi}^y \\ \Delta M_j^y \end{Bmatrix} = \left(\begin{bmatrix} S_{pi}^y & 0 \\ 0 & K_{jj}^y \end{bmatrix} + \frac{\begin{bmatrix} -S_{pi}^y \\ K_{ji}^y \end{bmatrix} \begin{bmatrix} S_{pi}^y & -K_{ij}^y \end{bmatrix}}{(S_{pi}^y + K_{ii}^y)} \right) \begin{Bmatrix} \Delta \theta_{pi}^y \\ \Delta \theta_j^y \end{Bmatrix} \quad (4.51)$$

$$\begin{Bmatrix} \Delta M_{pi}^z \\ \Delta M_j^z \end{Bmatrix} = \left(\begin{bmatrix} S_{pi}^z & 0 \\ 0 & K_{jj}^z \end{bmatrix} + \frac{\begin{bmatrix} -S_{pi}^z \\ K_{ji}^z \end{bmatrix} \begin{bmatrix} S_{pi}^z & -K_{ij}^z \end{bmatrix}}{(S_{pi}^z + K_{ii}^z)} \right) \begin{Bmatrix} \Delta \theta_{pi}^z \\ \Delta \theta_j^z \end{Bmatrix} \quad (4.52)$$

For plastic hinge at node j, we have:

$$\begin{Bmatrix} \Delta M_{ci}^y \\ \Delta M_j^y \end{Bmatrix} = \left(\begin{bmatrix} K_{ii}^y & 0 \\ 0 & S_{pj}^y \end{bmatrix} + \frac{\begin{bmatrix} K_{ij}^y \\ -S_{pj}^y \end{bmatrix} \begin{bmatrix} -K_{ji}^y & S_{pj}^y \end{bmatrix}}{(S_{pj}^y + K_{jj}^y)} \right) \begin{Bmatrix} \Delta \theta_i^y \\ \Delta \theta_{pj}^y \end{Bmatrix} \quad (4.53)$$

$$\begin{Bmatrix} \Delta M_{ci}^z \\ \Delta M_j^z \end{Bmatrix} = \left(\begin{bmatrix} K_{ii}^z & 0 \\ 0 & S_{pj}^z \end{bmatrix} + \frac{\begin{bmatrix} K_{ij}^z \\ -S_{pj}^z \end{bmatrix} \begin{bmatrix} -K_{ji}^z & S_{pj}^z \end{bmatrix}}{(S_{pj}^z + K_{jj}^z)} \right) \begin{Bmatrix} \Delta \theta_i^z \\ \Delta \theta_{pj}^z \end{Bmatrix} \quad (4.54)$$

The transformation matrices about y and x axes are given, respectively, by Equations 4.55 and 4.56.

$$[T_k^y]_{4 \times 2} = \begin{bmatrix} 1 & 0 \\ -1/L & -1/L \\ 0 & 1 \\ 1/L & 1/L \end{bmatrix} \quad (4.55)$$

$$[T_k^z]_{4 \times 2} = \begin{bmatrix} 1 & 0 \\ 1/L & 1/L \\ 0 & 1 \\ -1/L & -1/L \end{bmatrix} \quad (4.56)$$

This results in the eight degrees of freedom modified stiffness for flexural and shear in two bending planes, which will be superimposed on the remaining independent axial and torsional stiffness forming the modified element stiffness matrix accounting for the material yielding effect.

4.4.4 Modified Element Stiffness Matrix Accounting for Semi-Rigid Joints and Material Yielding

As explain in Sections 4.4.2 and 4.4.3, the effects of semi-rigid connection and section yielding are simulated by a pseudo-spring. These effects can be combined together by connecting their spring element to form a new resultant spring-in-series. This hybrid element is illustrated in Fig 4.9. The internal moments and rotations at each connection spring at deformed state are shown in Fig. 4.10, in which the inner pair of spring represents the yielding effect while the outer pair represents the connection flexibility effect.

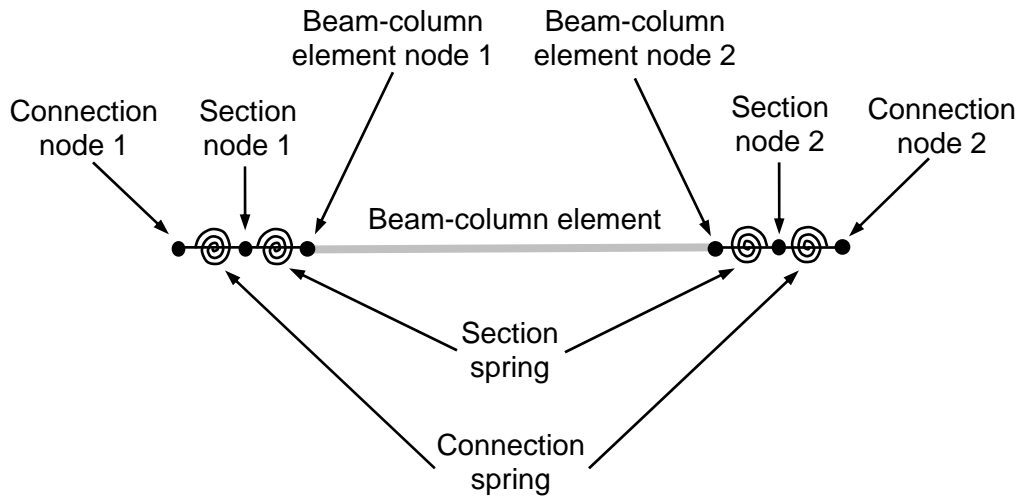


Fig. 4.9 Two spring-in-series hybrid element[1]

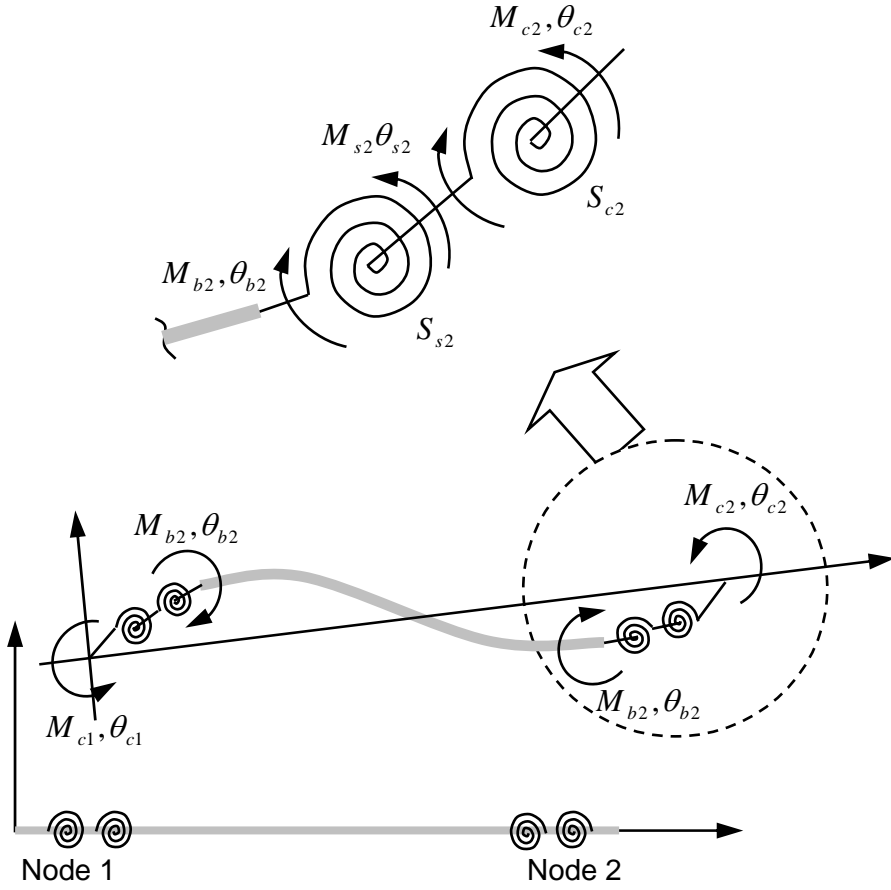


Fig. 4.10 Deformed beam-column element with 2 spring-in-series [1]

Considering six nodes hybrid element in Fig. 4.9, the moment rotation stiffness can be expressed as

$$\begin{Bmatrix} \Delta M_{c1} \\ \Delta M_{s1} \\ \Delta M_{b1} \\ \Delta M_{b2} \\ \Delta M_{s2} \\ \Delta M_{c2} \end{Bmatrix} = \begin{bmatrix} S_{c1} & -S_{c1} & 0 & 0 & 0 & 0 \\ -S_{c1} & S_{c1} + S_{s1} & -S_{s1} & 0 & 0 & 0 \\ 0 & -S_{s1} & S_{s1} + K_{11} & K_{12} & 0 & 0 \\ 0 & 0 & K_{21} & K_{22} + S_{s2} & -S_{s2} & 0 \\ 0 & 0 & 0 & -S_{s2} & S_{s2} + S_{c2} & -S_{c2} \\ 0 & 0 & 0 & 0 & -S_{c2} & S_{c2} \end{bmatrix} \begin{Bmatrix} \Delta \theta_{c1} \\ \Delta \theta_{s1} \\ \Delta \theta_{b1} \\ \Delta \theta_{b2} \\ \Delta \theta_{s2} \\ \Delta \theta_{c2} \end{Bmatrix} \quad (4.57)$$

where subscript ‘c’, ‘s’, and ‘b’ refer to connection, section, and beam-column element node, respectively. Also, S_{c1} , and S_{c2} are the End 1 and 2 tangent connection stiffnesses and S_{s1} , and S_{s2} are the end 1 and 2 section springs stiffnesses, respectively.

To derive a modified stiffness matrix, all loads are assumed to be applied at global node such that all the internal incremental moments are equal to zero. Then, the matrix can be condensed as follow:

$$\Delta M_{s1} = \Delta M_{s2} = \Delta M_{b1} = \Delta M_{b2} = 0 \quad (4.58)$$

By condensing the second and fifth row in the remaining rows in Equation 4.57, we have:

$$\begin{Bmatrix} \Delta M_{c1} \\ \Delta M_{b1} \\ \Delta M_{b2} \\ \Delta M_{c2} \end{Bmatrix} = \begin{bmatrix} S_{cs1} & -S_{cs1} & 0 & 0 \\ -S_{cs1} & S_{cs1} + K_{11} & K_{12} & 0 \\ 0 & K_{21} & K_{22} + S_{cs2} & -S_{cs2} \\ 0 & 0 & -S_{cs2} & S_{cs2} \end{bmatrix} \begin{Bmatrix} \Delta \theta_{c1} \\ \Delta \theta_{b1} \\ \Delta \theta_{b2} \\ \Delta \theta_{c2} \end{Bmatrix} \quad (4.59)$$

where:

$$S_{cs1} = \frac{S_{c1}S_{s1}}{S_{c1} + S_{s1}} \quad (4.60)$$

$$S_{cs2} = \frac{S_{c2}S_{s2}}{S_{c2} + S_{s2}} \quad (4.61)$$

Equation 4.59 has the same form as Equation 4.38, in which S_{cs1} , and S_{cs2} represent the combination of spring-in-series for connection and section spring. Subsequently, the internal moment at beam-column nodes can be condensed similar to procedures presented in Section 4.4.2 and 4.4.3.

4.5 Program Algorithm

The program implementation for each analysis type with and without considering joint flexibility and section yielding are explained in detail in this section. The three parameter kinematics hardening model have been employed for the semi-rigid joint. The equation of which is given by Equation 2.9. The section assemblage method takes into account the material yielding. For yielding effect, both elastic-plastic hinge and refine-plastic hinge are implemented in the program. Elastic-plastic hinge need less input parameters while refine-plastic hinge give more accurate result. As described in Section 2.4.3, all non-linear analysis in this study is implemented based on Newton-Raphson procedure because of its time efficiency and accuracy.

4.5.1 Linear Elastic Analysis

Step 1: Initialize required variables and parameters, i.e., node, element, connection parameters, degree of freedom.

Step 2: Calculate the element local stiffness matrix for each member $[k^e]$.

Step 3: If considered, modify stiffness matrix for accounting semi-rigid connection.

Step 4: Transform local stiffness to global stiffness matrix and assemble to form a system stiffness matrix.

$$[K] = \sum_{i=1}^{NELE} [k^g] = \sum_{i=1}^{NELE} [T]^T [k^e] [T]$$

Step 5: Calculate equivalent forces, then transform the force vector to global coordinate system and assemble to form a system force matrix.

$$\{F\} = \sum_{i=1}^{NELE} \{f^e\}$$

Step 6: Solve the system equilibrium for global displacement vector.

$$\{U\} = [K]^{-1} \{F\}$$

Step7: Extract the nodal displacement corresponding to degrees of freedom of each element and convert them to element local axis:

$$\{u^e\} = [T] \{u^g\}$$

Using element equilibrium equation, calculate element force vectors by using:

$$\{f^e\} = [k^e] \{u^e\}$$

4.5.2 Nonlinear Elastic and Inelastic Analysis by Newton-Raphson Method

Step 1: Initialize required variables and parameters, i.e., node, element, connection parameters, section parameter for yielding effect, degree of freedom, number of load step, and tolerance for force and displacement.

Step 2: Calculate equivalent forces in global coordinate system and assemble to form a system force matrix.

$$\{F\} = \sum_{i=1}^{NELE} \{f^g\}$$

Divide the force $\{F\}$, into incremental force $\{F_{inc}\}$ for each load step:

$$\{F_{inc}\} = \frac{\{F\}}{\text{number.of.loadsteps}}$$

Step 3: Calculate the element local stiffness matrix for each member $[k^e]$.

Step 4: If considered, modified stiffness matrix accounting semi-rigid connection and/or material yielding.

Step 5: Form the element tangent stiffness matrix, transform into global coordinate system and assemble to form a system tangent stiffness matrix.

$$[K_T] = \sum_{j=1}^{NELE} [k_T^s] = \sum_{j=1}^{NELE} [T]^T \left([k^e]_{12 \times 12} + [N] \right) [T]$$

where $[N]$ are formulated from accumulated member force in local coordinate system. For the first iteration of first load step, $[N]$ is equal to zero due to no member force at the initial.

Step 6: Solve the incremental system equilibrium equation for displacement vector:

$$\text{For first iterations, } \{\Delta U\}_1 = [K]^{-1} \{F_{inc}\}$$

$$\text{For other iterations, } \{\Delta U\}_{i+1} = [K]^{-1} \{\Delta F\}_{i+1}$$

Step 7: Accumulate the displacement increment to total displacement.

$$\{U\}_{i+1} = \{U\}_i + \{\Delta U\}_{i+1}$$

Step 8: Update the geometry, using updated Lagrangian formulation as follows

$$\{x\}_{i+1} = \{x\}_i + \{\Delta u\}_{i+1}$$

Step 9: Transform global displacement vector to element local displacement vector.

$$\{\Delta u^e\}_{i+1} = [T] \{\Delta u^g\}_{i+1}$$

Step 11: Calculate incremental resultant forces and accumulate to obtain the member forces.

$$\{\Delta r^e\}_{i+1} = [k_T^e]_{i+1} \{\Delta u^e\}_{i+1}$$

$$\{r_{total}^e\}_{i+1} = \{r_{total}^e\}_i + \{\Delta r^e\}_{i+1}$$

Step 12: Transform local resultant forces to be global coordinate system and assemble them to form a system resultant force.

$$\{R_{total}\}_{i+1} = \sum_{j=1}^{NELE} \{r_{total}^g\}_{i+1} = \sum_{j=1}^{NELE} [T]^T \{r_{total}^e\}_{i+1}$$

Step 13: Accumulate applied forces to form total applied force vector:

$$\{F_{total}\}_{i+1} = \{F_{total}\}_i + \{F\}_{i+1}$$

Step 14: Determined the unbalanced force vector:

$$\{\Delta F\}_{i+1} = \{F_{total}\}_{i+1} - \{R_{total}\}_{i+1}$$

Step 15: Check for equilibrium.

$$\{\Delta F\}^T \{\Delta F\} < Tolerance \times \{R\}^T \{R\}$$

$$\{\Delta U\}^T \{\Delta U\} < Tolerance \times \{U\}^T \{U\}$$

If these two equations are satisfied, applied next load step. Otherwise, continue to the next iteration. All calculations are repeated from step 3-14 until the results of last load step are satisfied.

CHAPTER V

PROGRAM VERIFICATIONS

5.1 Program Algorithm Verification

The behavior of structures with different connection types are examined and the load deflection curve for each of them are compared. In this study, the three dimensional two stories space frames with two different load cases representing in Fig. 5.1 and 5.2 below are used.

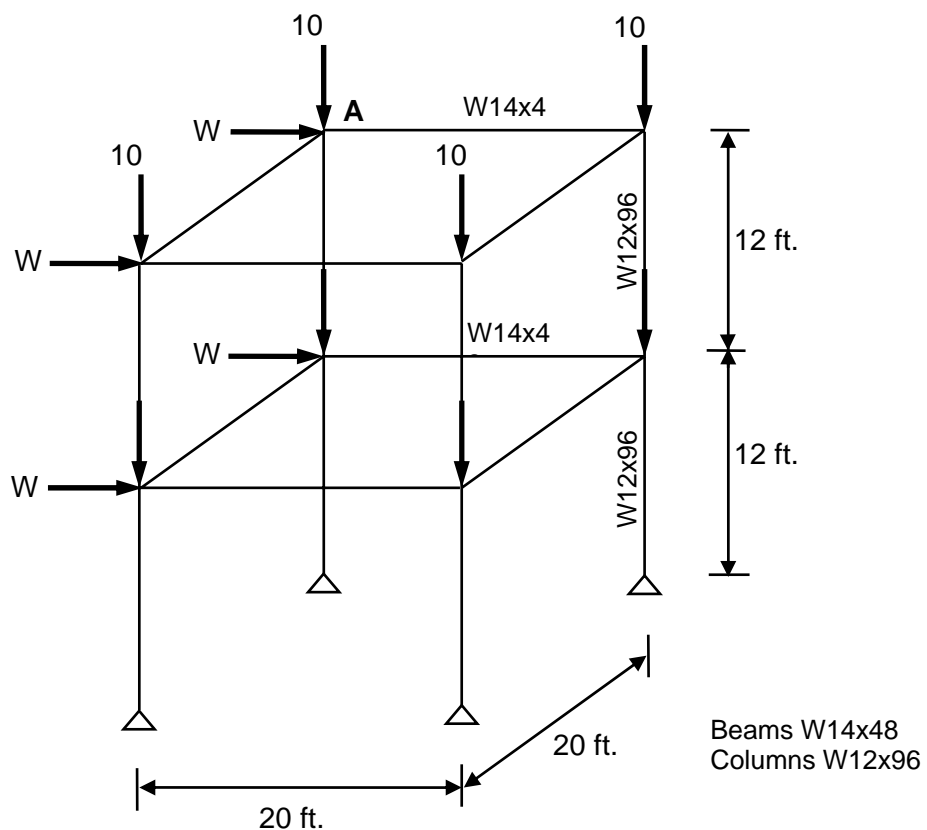


Fig. 5.1 Example Frame 1

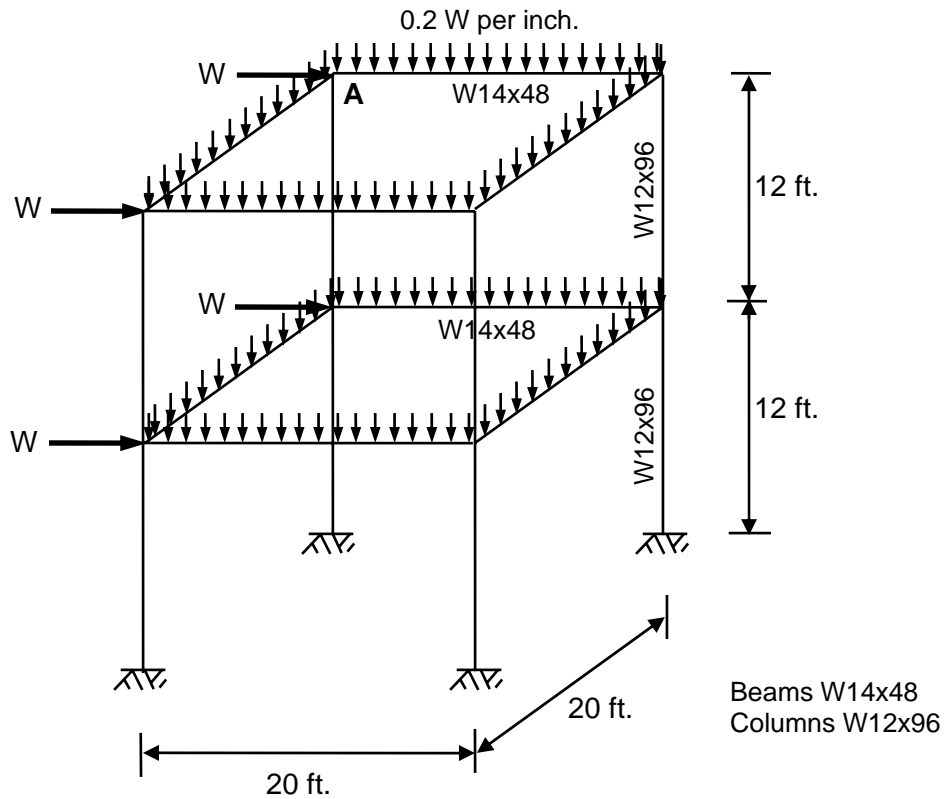


Fig. 5.2 Example Frame 2

The tests are performed with different connection stiffness in both linear and non-linear analysis to obtain the relationship of flexural behavior of structure for several connection types. Since the results for all tests are compared, all required constant input parameters for material properties including plasticity effects are set to be the same for all cases and have been shown in Table 5.1 as follow

Table 5.1 Material properties parameters used in the program verification

Parameter	Value
Poisson's ratio	0.3
Young modulus	29000 ksi
Yield stress	36 ksi
Maximum residual stress	18 ksi

5.2 Semi-Rigid Connection Parameters

To verify the results of the program, load-deflection curves for different types of connections have been conducted to represent the relationships of connection flexural stiffness and non-linearity behavior. The required parameters for kinematic hardening model, which is the connection model employed in this research, are assumed from the experimental data for four connection types, i.e., single web angle, double web angle, top and seat angle and top and seat with double web angle. These parameters are listed in Table 5.2 and will be used through this verification.

Table 5.2 Semi-rigid connection parameters used in the program verification

	S_c^0	S_h	θ_0	n
Single-web angle	100000	30000	0.005	1.0945
Double-web angle	200000	60000	0.005	0.91
Top- and seat-angle (without Double-web angle)	800000	240000	0.0025	0.9933
Top- and seat-angle (with Double-web angle)	2000000	60000	0.003	1.0167

5.3 Behavior of Semi-Rigid Connections in Linear Analysis

To compare the flexure behavior of four connection types in Table 5.2, The tests have been performed on two two-stories frames in Fig. 5.1 and 5.2 by increasing the value of loads, W , to calculate maximum deflection at point A. Using lateral displacements of point A in the direction of applied load, the results of rigid analyses are compared in Fig. 5.3 and Fig. 5.4 when properties of connections of Table 5.2 used as semi-rigid connection in 3-D frames of Fig. 5.1 and 5.2, respectively.

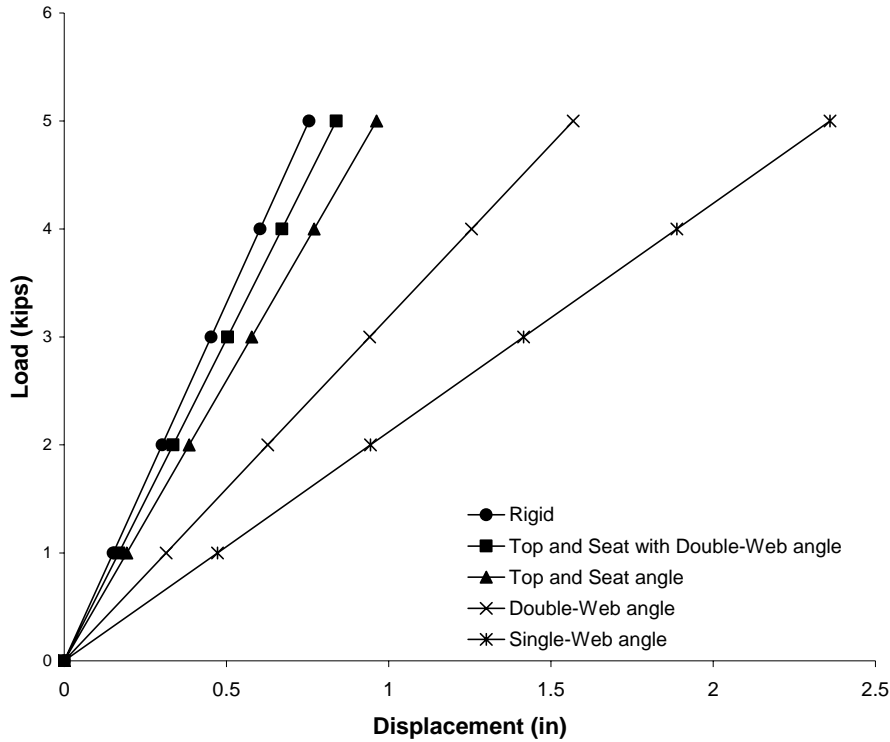


Fig. 5.3 Load-displacement curves in linear analysis of Frame 1(Fig. 5.1)

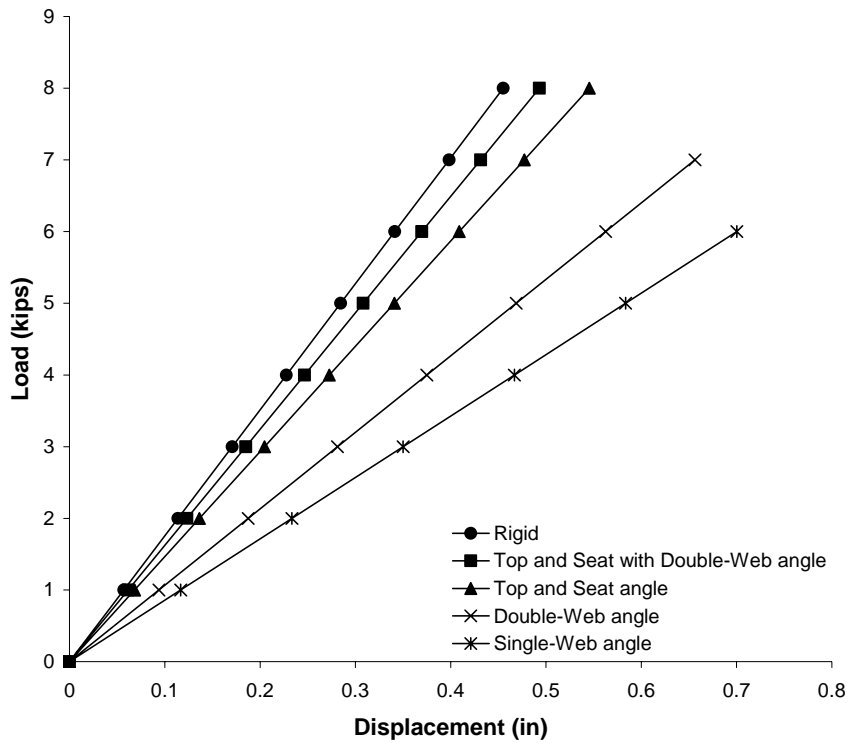


Fig. 5.4 Load-displacement curves in linear analysis of Frame 2(Fig. 5.2)

As illustrated in the aforementioned, both frames behave linearly with increasing loads. Also, the lateral sway increases as connection stiffness decreases, which is an indication that the developed algorithm traces the behavioral path of the frame.

5.4 Behavior of Semi-Rigid Connections in Non-linear Analysis

The non-linear behaviors of two frames in Fig. 5.1 and 5.2 are examined using the same condition as those used for linear analysis in the previous section. In each type of connection, the lateral deflection of Point A and loads, W , are plotted and presented in Fig. 5.5-5.6.

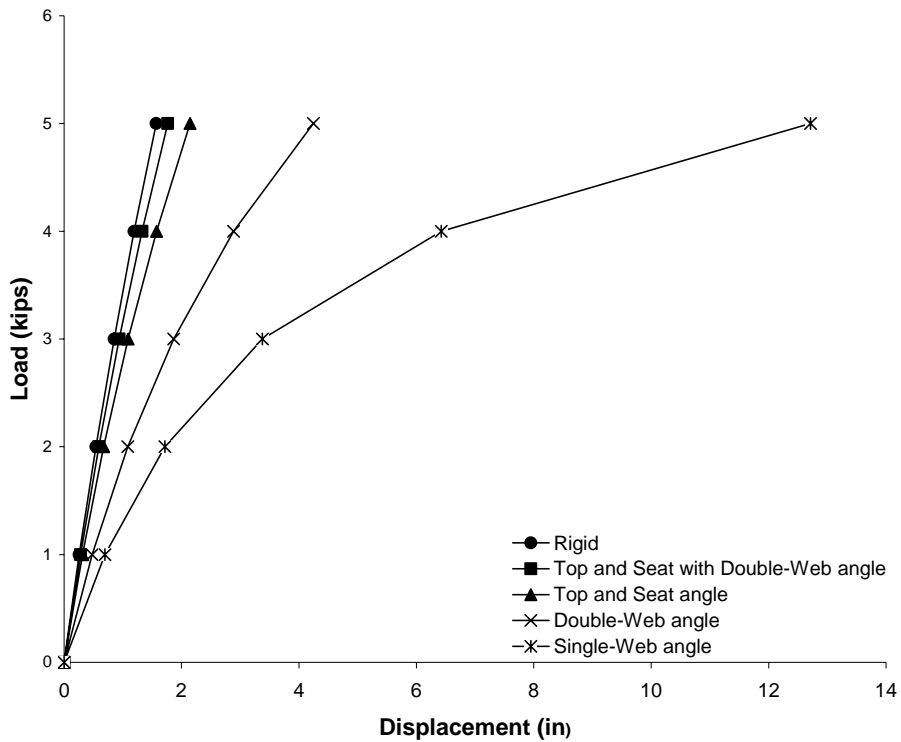


Fig. 5.5 Load-displacement curves in non-linear analysis of Frame 1(Fig. 5.1)

These Figures indicate that the algorithm presented follows the expected behavior. For example, the nonlinear analysis, which includes both $P-\delta$ and $P-\Delta$, analyses, results in a stiffer structure for the rigid case. As shown in the figure, as the connection stiffness decreases, the lateral sway would increase, which introduce a more flexible system. Figure 5.5 and 5.6 indicate that when rigid and single web angle connections are used in the 3-D frame of Figure 5.1 and 5.2, the lateral sways are minimum and maximum, respectively.

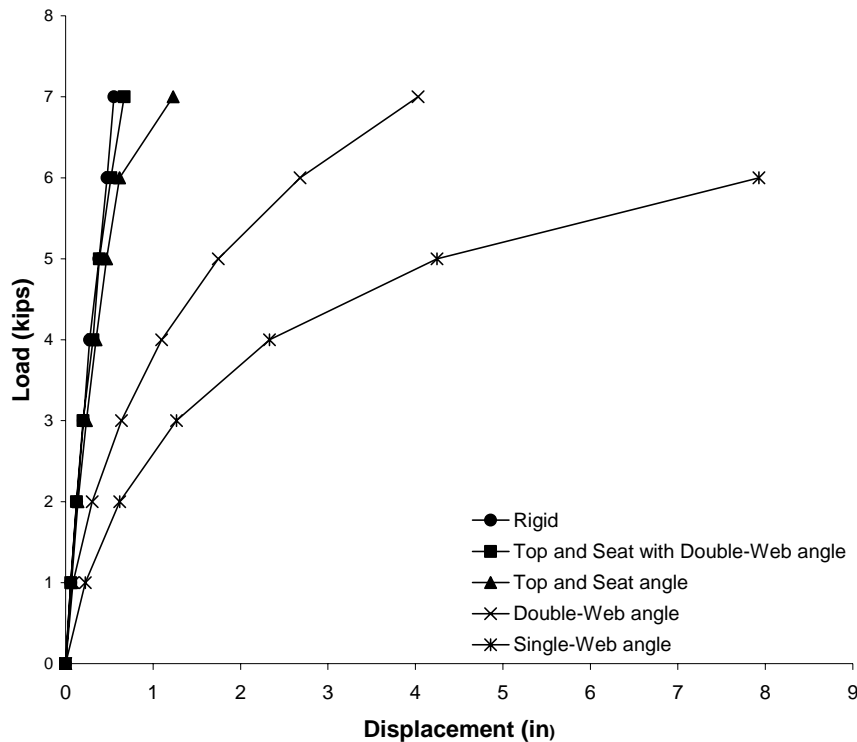


Fig. 5.6 Load-displacement curves in non-linear analysis of Frame 2(Fig. 5.2)

5.5 Web-Based Representation

This algorithm is developed for real-time Web-based analysis of three-dimensional frames with semi-rigid joints. The complete Web-based can be visited online at enterprise.uta.edu/3dframe/frame.htm . An example of the Web-based output is given in Fig. 5.8 and 5.9 for graphical and tabulated representations, respectively.

Frame 2 in Fig. 5.2 is used as input frame structure in which lateral wind loads, W , are 5 kips, and distributed loads on each beam components are 1 kips/inches. The node and element numbering assigned in this implementation are shown in Fig. 5.7. The top- and seat-angle connection parameters in Table 5.2 are assumed to be used in all beam-to-column joint to compare the results with those of rigid connections. In

addition, the effect of sectional yielding by elastic-plastic hinge method is also included in the analysis.

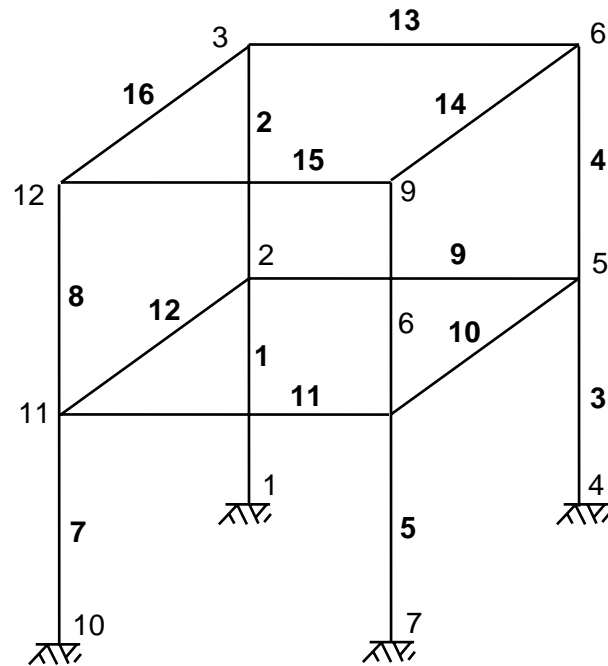


Fig. 5.7 Node and element numbering of Frame 2 (Fig. 5.2) for web-based example

The input data for node, element, load, connection and yielding parameters are shown in Table 5.3-5.7 as follows:

Table 5.3 Node input of Frame 2 for Web-based example

Node Data				
Item	x-Coor	y-Coor	z-Coor	Type
1	0	0	0	Fix
2	0	144	0	Free
3	0	288	0	Free
4	240	0	0	Fix
5	240	144	0	Free
6	240	288	0	Free
7	240	0	240	Fix
8	240	144	240	Free
9	240	288	240	Free
10	0	0	240	Fix
11	0	144	240	Free
12	0	288	240	Free

Table 5.4 Element input of Frame 2 for Web-based example

Element Data									
Item	Type	Node 1	Node 2	A	E	Iy	Iz	J	Poisson.
1	Column	1	2	28.2	29000	270	833	6.86	0.3
2	Column	2	3	28.2	29000	270	833	6.86	0.3
3	Column	4	5	28.2	29000	270	833	6.86	0.3
4	Column	5	6	28.2	29000	270	833	6.86	0.3
5	Column	7	8	28.2	29000	270	833	6.86	0.3
6	Column	8	9	28.2	29000	270	833	6.86	0.3
7	Column	10	11	28.2	29000	270	833	6.86	0.3
8	Column	11	12	28.2	29000	270	833	6.86	0.3
9	Beam	2	5	14.1	29000	51.4	485	1.46	0.3
10	Beam	5	8	14.1	29000	51.4	485	1.46	0.3
11	Beam	8	11	14.1	29000	51.4	485	1.46	0.3
12	Beam	11	2	14.1	29000	51.4	485	1.46	0.3
13	Beam	3	6	14.1	29000	51.4	485	1.46	0.3
14	Beam	6	9	14.1	29000	51.4	485	1.46	0.3
15	Beam	9	12	14.1	29000	51.4	485	1.46	0.3
16	Beam	12	3	14.1	29000	51.4	485	1.46	0.3

Table 5.5 Load input of Frame 2 for Web-based example

Load Data							
Item	Elem ID	Type	Dir.	Load 1	Dist 1	Load 2	Dist 2
1	1	Conc. Lateral	Global x	5	144	0	0
2	2	Conc. Lateral	Global x	5	144	0	0
3	7	Conc. Lateral	Global x	5	144	0	0
4	8	Conc. Lateral	Global x	5	144	0	0
5	9	Dist. Lateral	Global y	-1	0	-1	240
6	10	Dist. Lateral	Global y	-1	0	-1	240
7	11	Dist. Lateral	Global y	-1	0	-1	240
8	12	Dist. Lateral	Global y	-1	0	-1	240
9	13	Dist. Lateral	Global y	-1	0	-1	240
10	14	Dist. Lateral	Global y	-1	0	-1	240
11	15	Dist. Lateral	Global y	-1	0	-1	240
12	16	Dist. Lateral	Global y	-1	0	-1	240

Table 5.6 Connection parameter input of Frame 2 for Web-based example

Element Connection Data								
Elem ID	Rki1	Rb1	Oo1	n1	Rki2	Rb2	Oo2	n2
9	800000	240000	0.0025	0.9933	800000	240000	0.0025	0.9933
10	800000	240000	0.0025	0.9933	800000	240000	0.0025	0.9933
11	800000	240000	0.0025	0.9933	800000	240000	0.0025	0.9933
12	800000	240000	0.0025	0.9933	800000	240000	0.0025	0.9933
13	800000	240000	0.0025	0.9933	800000	240000	0.0025	0.9933
14	800000	240000	0.0025	0.9933	800000	240000	0.0025	0.9933
15	800000	240000	0.0025	0.9933	800000	240000	0.0025	0.9933
16	800000	240000	0.0025	0.9933	800000	240000	0.0025	0.9933

Table 5.7 Yielding parameter input of Frame 2 for Web-based example

Element Yielding data							
Elem ID	Type	t	T	d	D	B	6y
9	Elas.	0.34	0.595	12.6	13.79	8.03	36
10	Elas.	0.34	0.595	12.6	13.79	8.03	36
11	Elas.	0.34	0.595	12.6	13.79	8.03	36
12	Elas.	0.34	0.595	12.6	13.79	8.03	36
13	Elas.	0.34	0.595	12.6	13.79	8.03	36
14	Elas.	0.34	0.595	12.6	13.79	8.03	36
15	Elas.	0.34	0.595	12.6	13.79	8.03	36
16	Elas.	0.34	0.595	12.6	13.79	8.03	36

Fig 5.8 shows the initial geometry of Frame 2 with two springs in series at both ends of each beam to take into account the effect of material nonlinearity and plastic yielding. The visualized graphical input and output are represented in oblique parallel projection views to maintain the proportions of the objects of which the angle between the oblique projection line and the line on the view plane is assigned to be 30 degrees.

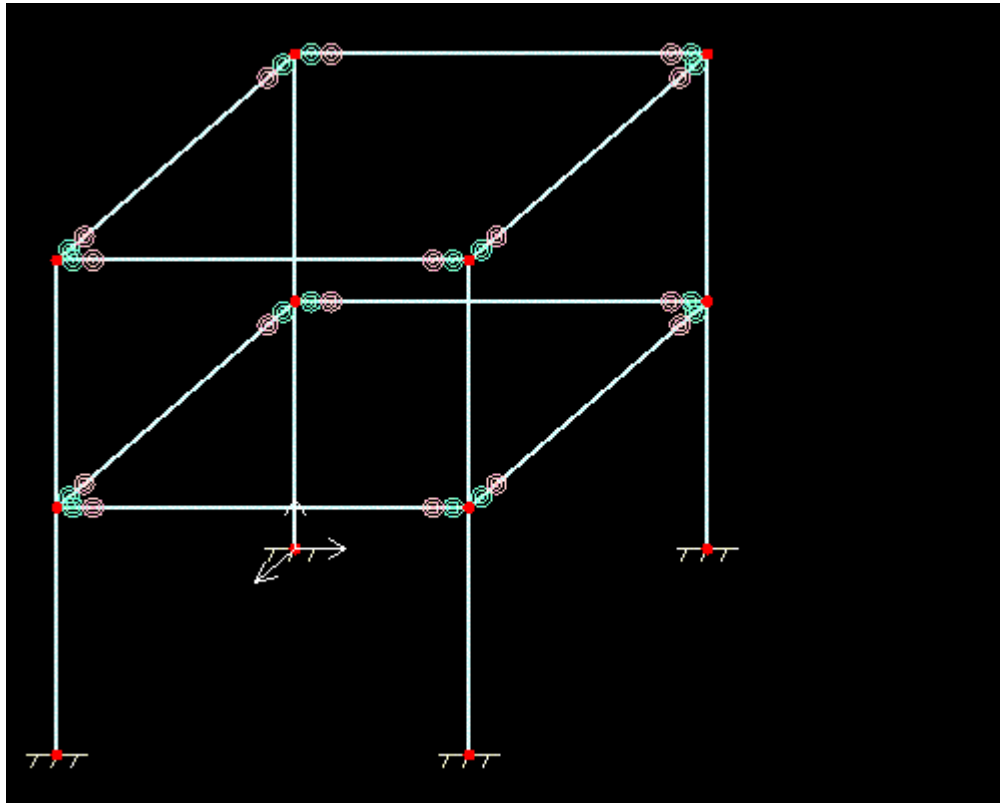


Fig. 5.8 Initial geometry of Frame 2 for Web-based example

The deformed geometry of non-linear inelastic semi-rigid analysis are shown in Fig. 5.9 compared to the initial geometry. The deflection multiplication factor indicated at the bottom of the picture allow to represent the shape of the deform structures in which the maximum deflection shown in graphical view is set to a constant number. As a result, the deformed shape of structures can be visualized for every load cased. For example, when the maximum deflection is a very small number compare to the size of structure, the actual views in initial and deformed geometry of the whole structure are almost the same. To visualized the deformation of the structure in this case, the maximum deflection of output image are set to be constant which result in a very large

value of deflection multiplication factor. As illustrated in fig. 5.9, the actual deflection of structure is 38 times less than the graphical output representation.

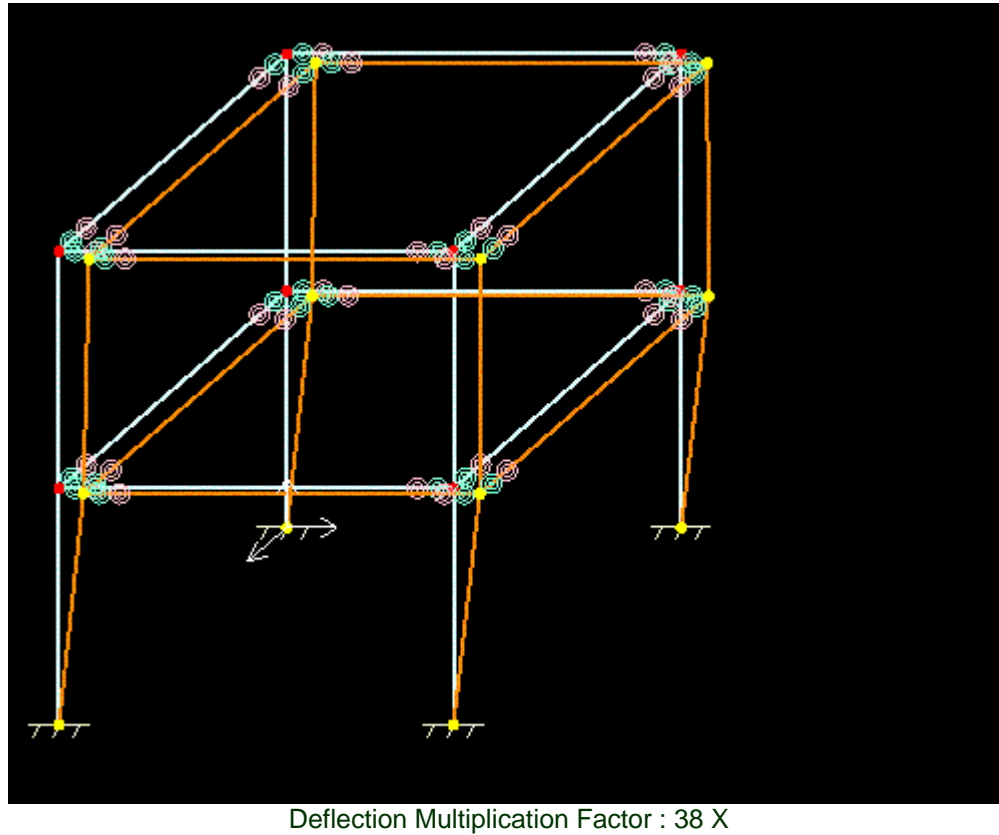


Fig. 5.9 Deform geometry of Frame 2 for Web-based example in Nonlinear inelastic semi-rigid analysis

With the same structure and applied forces, the non-linear inelastic and elastic analyses have been tested for both rigid and semi-rigid connection conditions. Results for nodal displacements and member forces of Frame 2 are tabulated in Tables 5.8 and 5.12.

Table 5.8 Deformed geometry in non-linear elastic analysis of Frame 2 with rigid connections.

Deformed Element Data in Global Coordinate							
Elem.	Elem. Node	x Disp.	y Disp.	z Disp.	x Rotat.	y Rotat.	z Rotat.
1	1	0	0	0	0	0	0
	2	0.3219	-0.084331	-0.008491	0.0048662	0.00020144	-0.009356
2	1	0.3219	-0.084331	-0.008491	0.0048662	0.00020144	-0.009356
	2	0.38187	-0.12593	0.018125	0.015351	0.000032284	-0.016856
3	1	0	0	0	0	0	0
	2	0.34849	-0.086744	-0.0106	0.0048377	0.00021138	0.0067426
4	1	0.34849	-0.086744	-0.0106	0.0048377	0.00021138	0.0067426
	2	0.3408	-0.12923	0.019138	0.014071	0.000020503	0.015039
5	1	0	0	0	0	0	0
	2	0.34849	-0.086744	0.0106	-0.004838	-0.00021138	0.0067426
6	1	0.34849	-0.086744	0.0106	-0.004838	-0.00021138	0.0067426
	2	0.3408	-0.12923	-0.019138	-0.014071	-2.0504E-05	0.015039
7	1	0	0	0	0	0	0
	2	0.3219	-0.084331	0.0084911	-0.004866	-0.00020144	-0.009356
8	1	0.3219	-0.084331	0.0084911	-0.004866	-0.00020144	-0.009356
	2	0.38187	-0.12593	-0.018125	-0.015351	-3.2285E-05	-0.016856
9	1	0.3219	-0.084331	-0.008491	0.0048662	0.00020144	-0.009356
	2	0.34849	-0.086744	-0.0106	0.0048377	0.00021138	0.0067426
10	1	0.34849	-0.086744	-0.0106	0.0048377	0.00021138	0.0067426
	2	0.34849	-0.086744	0.0106	-0.004838	-0.00021138	0.0067426
11	1	0.34849	-0.086744	0.0106	-0.004838	-0.00021138	0.0067426
	2	0.3219	-0.084331	0.0084911	-0.004866	-0.00020144	-0.009356
12	1	0.3219	-0.084331	0.0084911	-0.004866	-0.00020144	-0.009356
	2	0.3219	-0.084331	-0.008491	0.0048662	0.00020144	-0.009356
13	1	0.38187	-0.12593	0.018125	0.015351	0.000032284	-0.016856
	2	0.3408	-0.12923	0.019138	0.014071	0.000020503	0.015039
14	1	0.3408	-0.12923	0.019138	0.014071	0.000020503	0.015039
	2	0.3408	-0.12923	-0.019138	-0.014071	-2.0504E-05	0.015039
15	1	0.3408	-0.12923	-0.019138	-0.014071	-2.0504E-05	0.015039
	2	0.38187	-0.12593	-0.018125	-0.015351	-3.2285E-05	-0.016856
16	1	0.38187	-0.12593	-0.018125	-0.015351	-3.2285E-05	-0.016856
	2	0.38187	-0.12593	0.018125	0.015351	0.000032284	-0.016856

Table 5.9 Member forces in non-linear elastic analysis of Frame 2
with rigid connections

Element Force Data in Global Coordinate							
Elem.	Elem. Node	F-x	F-y	F-z	Ro-x	Ro-y	Ro-z
1	1	14.693	473.58	32.774	1572.1	-4.7624	-360.65
	2	-14.693	-473.58	-32.774	3151.4	-9.2877	-1487.2
2	1	64.986	237.37	61.765	3478.3	-0.51771	-4313.6
	2	-64.986	-237.37	-61.765	5400.2	-1.626	-5015.5
3	1	-24.693	486.42	29.181	1401.3	-4.5816	1562.1
	2	24.693	-486.42	-29.181	2807.4	-8.9505	2288.7
4	1	-69.986	242.63	65.235	3825.6	-1.1017	4423.9
	2	69.986	-242.63	-65.235	5550.4	-1.3331	5645.2
5	1	-24.693	486.42	-29.181	-1401.3	4.5816	1562.1
	2	24.693	-486.42	29.181	-2807.4	8.9505	2288.7
6	1	-69.986	242.63	-65.235	-3825.6	1.1017	4423.9
	2	69.986	-242.63	65.235	-5550.4	1.3331	5645.2
7	1	14.693	473.58	-32.774	-1572.1	4.7624	-360.65
	2	-14.693	-473.58	32.774	-3151.4	9.2877	-1487.2
8	1	64.986	237.37	-61.765	-3478.3	0.51771	-4313.6
	2	-64.986	-237.37	61.765	-5400.2	1.626	-5015.5
9	1	-45.293	-3.7976	-0.060529	-0.020097	7.3035	-1399.2
	2	45.293	3.7976	0.060529	0.0055766	7.427	487.43
10	1	-9.712E-10	-5.128E-07	-36.115	566.94	2.6252	1.6415E-09
	2	9.7122E-10	5.1282E-07	36.115	-566.94	-2.6252	-1.642E-09
11	1	45.293	3.7976	-0.060529	-0.005577	-7.427	487.43
	2	-45.293	-3.7976	0.060529	0.020097	-7.3035	-1399.2
12	1	-2.322E-09	-1.334E-07	28.93	-570.29	-2.5019	3.324E-08
	2	2.3215E-09	1.3337E-07	-28.93	570.29	2.5019	-3.324E-08
13	1	69.986	-2.626	-0.00897	0.10389	1.2249	-2184.5
	2	-69.986	2.626	0.0089697	-0.098824	1.0784	1554.8
14	1	-1.804E-08	4.9846E-07	65.226	1649.7	0.25474	-1.553E-08
	2	1.8041E-08	-4.985E-07	-65.226	-1649.7	-0.25473	1.5534E-08
15	1	-69.986	2.626	-0.00897	0.098824	-1.0784	1554.8
	2	69.986	-2.626	0.0089698	-0.10389	-1.2249	-2184.5
16	1	1.0305E-08	8.3504E-08	-61.774	-1799.7	-0.40112	1.481E-07
	2	-1.031E-08	-8.35E-08	61.774	1799.7	0.40112	-1.481E-07

Table 5.10 Deformed geometry in non-linear elastic analysis of Frame 2
with Top- and Seat-angle connections

Deformed Element Data in Global Coordinate							
Elem.	Elem. Node	x Disp.	y Disp.	z Disp.	x Rotat.	y Rotat.	z Rotat.
1	1	0	0	0	0	0	0
	2	0.3964	-0.084877	-0.010124	0.0047158	0.00022184	-0.01028
2	1	0.3964	-0.084877	-0.010124	0.0047158	0.00022184	-0.01028
	2	0.46811	-0.1264	0.019485	0.015493	0.000029912	-0.019409
3	1	0	0	0	0	0	0
	2	0.42538	-0.087285	-0.011673	0.0047554	0.00023163	0.0058605
4	1	0.42538	-0.087285	-0.011673	0.0047554	0.00023163	0.0058605
	2	0.42459	-0.12983	0.020095	0.015354	0.000016905	0.01479
5	1	0	0	0	0	0	0
	2	0.42538	-0.087285	0.011673	-0.004755	-0.00023163	0.0058605
6	1	0.42538	-0.087285	0.011673	-0.004755	-0.00023163	0.0058605
	2	0.42459	-0.12983	-0.020095	-0.015354	-1.6905E-05	0.01479
7	1	0	0	0	0	0	0
	2	0.3964	-0.084877	0.010124	-0.004716	-0.00022184	-0.01028
8	1	0.3964	-0.084877	0.010124	-0.004716	-0.00022184	-0.01028
	2	0.46811	-0.1264	-0.019485	-0.015493	-2.9912E-05	-0.019409
9	1	0.3964	-0.084877	-0.010124	0.0047158	0.00022184	-0.01028
	2	0.42538	-0.087285	-0.011673	0.0047554	0.00023163	0.0058605
10	1	0.42538	-0.087285	-0.011673	0.0047554	0.00023163	0.0058605
	2	0.42538	-0.087285	0.011673	-0.004755	-0.00023163	0.0058605
11	1	0.42538	-0.087285	0.011673	-0.004755	-0.00023163	0.0058605
	2	0.3964	-0.084877	0.010124	-0.004716	-0.00022184	-0.01028
12	1	0.3964	-0.084877	0.010124	-0.004716	-0.00022184	-0.01028
	2	0.3964	-0.084877	-0.010124	0.0047158	0.00022184	-0.01028
13	1	0.46811	-0.1264	0.019485	0.015493	0.000029912	-0.019409
	2	0.42459	-0.12983	0.020095	0.015354	0.000016905	0.01479
14	1	0.42459	-0.12983	0.020095	0.015354	0.000016905	0.01479
	2	0.42459	-0.12983	-0.020095	-0.015354	-1.6905E-05	0.01479
15	1	0.42459	-0.12983	-0.020095	-0.015354	-1.6905E-05	0.01479
	2	0.46811	-0.1264	-0.019485	-0.015493	-2.9912E-05	-0.019409
16	1	0.46811	-0.1264	-0.019485	-0.015493	-2.9912E-05	-0.019409
	2	0.46811	-0.1264	0.019485	0.015493	0.000029912	-0.019409

Table 5.11 Deformed geometry in non-linear inelastic analysis of Frame 2
with rigid connections

Deformed Element Data in Global Coordinate							
Elem.	Elem. Node	x Disp.	y Disp.	z Disp.	x Rotat.	y Rotat.	z Rotat.
1	1	0	0	0	0	0	0
	2	0.3219	-0.084331	-0.008491	0.0048662	0.00020144	-0.009356
2	1	0.3219	-0.084331	-0.008491	0.0048662	0.00020144	-0.009356
	2	0.38187	-0.12593	0.018125	0.015351	0.000032281	-0.016856
3	1	0	0	0	0	0	0
	2	0.34849	-0.086744	-0.0106	0.0048378	0.00021138	0.0067426
4	1	0.34849	-0.086744	-0.0106	0.0048378	0.00021138	0.0067426
	2	0.3408	-0.12923	0.019138	0.014071	0.000020501	0.015039
5	1	0	0	0	0	0	0
	2	0.34849	-0.086744	0.0106	-0.004838	-0.00021138	0.0067426
6	1	0.34849	-0.086744	0.0106	-0.004838	-0.00021138	0.0067426
	2	0.3408	-0.12923	-0.019137	-0.014071	-2.0506E-05	0.015039
7	1	0	0	0	0	0	0
	2	0.3219	-0.084331	0.008491	-0.004866	-0.00020144	-0.009356
8	1	0.3219	-0.084331	0.008491	-0.004866	-0.00020144	-0.009356
	2	0.38187	-0.12593	-0.018125	-0.015351	-3.2287E-05	-0.016856
9	1	0.3219	-0.084331	-0.008491	0.0048662	0.00020144	-0.009356
	2	0.34849	-0.086744	-0.0106	0.0048378	0.00021138	0.0067426
10	1	0.34849	-0.086744	-0.0106	0.0048378	0.00021138	0.0067426
	2	0.34849	-0.086744	0.0106	-0.004838	-0.00021138	0.0067426
11	1	0.34849	-0.086744	0.0106	-0.004838	-0.00021138	0.0067426
	2	0.3219	-0.084331	0.008491	-0.004866	-0.00020144	-0.009356
12	1	0.3219	-0.084331	0.008491	-0.004866	-0.00020144	-0.009356
	2	0.3219	-0.084331	-0.008491	0.0048662	0.00020144	-0.009356
13	1	0.38187	-0.12593	0.018125	0.015351	0.000032281	-0.016856
	2	0.3408	-0.12923	0.019138	0.014071	0.000020501	0.015039
14	1	0.3408	-0.12923	0.019138	0.014071	0.000020501	0.015039
	2	0.3408	-0.12923	-0.019137	-0.014071	-2.0506E-05	0.015039
15	1	0.3408	-0.12923	-0.019137	-0.014071	-2.0506E-05	0.015039
	2	0.38187	-0.12593	-0.018125	-0.015351	-3.2287E-05	-0.016856
16	1	0.38187	-0.12593	-0.018125	-0.015351	-3.2287E-05	-0.016856
	2	0.38187	-0.12593	0.018125	0.015351	0.000032281	-0.016856

Table 5.12 Deformed geometry in non-linear inelastic analysis of Frame 2
With Top- and Seat

. -angle connections

Deformed Element Data in Global Coordinate							
Elem.	Elem. Node	x Disp.	y Disp.	z Disp.	x Rotat.	y Rotat.	z Rotat.
1	1	0	0	0	0	0	0
	2	0.39616	-0.084875	-0.010197	0.0047497	0.01047	-0.010284
2	1	0.39616	-0.084875	-0.010197	0.0047497	0.01047	-0.010284
	2	0.46803	-0.1264	0.019514	0.015485	0.00013736	-0.019407
3	1	0	0	0	0	0	0
	2	0.42513	-0.087283	-0.011721	0.0047916	0.01068	0.0058651
4	1	0.42513	-0.087283	-0.011721	0.0047916	0.01068	0.0058651
	2	0.42452	-0.12983	0.02011	0.015338	0.00012868	0.014785
5	1	0	0	0	0	0	0
	2	0.42513	-0.087283	0.011721	-0.004792	-0.01068	0.0058651
6	1	0.42513	-0.087283	0.011721	-0.004792	-0.01068	0.0058651
	2	0.42452	-0.12983	-0.02011	-0.015338	-0.00012868	0.014785
7	1	0	0	0	0	0	0
	2	0.39616	-0.084875	0.010197	-0.00475	-0.01047	-0.010284
8	1	0.39616	-0.084875	0.010197	-0.00475	-0.01047	-0.010284
	2	0.46803	-0.1264	-0.019514	-0.015485	-0.00013736	-0.019407
9	1	0.39616	-0.084875	-0.010197	0.0047497	0.01047	-0.010284
	2	0.42513	-0.087283	-0.011721	0.0047916	0.01068	0.0058651
10	1	0.42513	-0.087283	-0.011721	0.0047916	0.01068	0.0058651
	2	0.42513	-0.087283	0.011721	-0.004792	-0.01068	0.0058651
11	1	0.42513	-0.087283	0.011721	-0.004792	-0.01068	0.0058651
	2	0.39616	-0.084875	0.010197	-0.00475	-0.01047	-0.010284
12	1	0.39616	-0.084875	0.010197	-0.00475	-0.01047	-0.010284
	2	0.39616	-0.084875	-0.010197	0.0047497	0.01047	-0.010284
13	1	0.46803	-0.1264	0.019514	0.015485	0.00013736	-0.019407
	2	0.42452	-0.12983	0.02011	0.015338	0.00012868	0.014785
14	1	0.42452	-0.12983	0.02011	0.015338	0.00012868	0.014785
	2	0.42452	-0.12983	-0.02011	-0.015338	-0.00012868	0.014785
15	1	0.42452	-0.12983	-0.02011	-0.015338	-0.00012868	0.014785
	2	0.46803	-0.1264	-0.019514	-0.015485	-0.00013736	-0.019407
16	1	0.46803	-0.1264	-0.019514	-0.015485	-0.00013736	-0.019407
	2	0.46803	-0.1264	0.019514	0.015485	0.00013736	-0.019407

CHAPTER VI

SUMMARY, CONCLUSIONS, AND RECOMMENDATIONS

6.1 Summary

The nonlinear behavior of connections caused by the second order effects of geometric change and material yielding, governs the load-carrying capacity of frame structures. These non-linearity effects significantly alter analysis results. This research developed a Web-based 3-D semi-rigid frame analysis algorithm to incorporate both the geometric and the material nonlinearities.

The Web-based computer program is developed to include coupled nonlinear effects such as connection, geometric, and material nonlinearities using Web-based C# language. The semi-rigid behavior of the connections are included in the analysis in which the kinematic hardening model equation is employed for non-linear implementation. Also, yielding effects in inelastic analysis are formulated based on the section assemblage concept. The effects of nonlinear behavior of connection and/or material yielding are included in the analysis using the concept of connecting pseudo spring elements at the end of beam so that the stiffness of the beam is modified. The non-linear computational procedures are based on the Newton-Raphson method in which the tangent stiffness is used.

To visualize the frame structure in web-based application analysis program, the algorithm is performed to represent the input and output in graphical images. The three dimensional drawing is generated using oblique parallel projection view to show the initial and deformed geometries of the structure.

6.2 Conclusions

The Web-based three dimensional semi-rigid frame analysis program was developed successfully. This algorithm is capable of considering connection, geometric, and material nonlinearity.

A three dimensional rigid joint analysis was conducted. The result of which were verified with STADD PRO software. The lateral deflections and member forces were compared in this analysis.

In order to further validate the algorithm presented, a validation study was conducted in Chapter 5, in which the connection stiffness to the semi-rigid connections in the frame was varied from a low to intermediate to high and the frame response was recorded. The lateral sway and member forces followed the expected trend. The results of this analysis is presented in both graphical and tabulated form.

6.3 Recommendation

For further studies, it is recommended that a detailed parametric study be conducted to:

1. Identify the effect of different connections with different initial and post-yield stiffness on the overall frame behavior. Traditionally, same types of connection have been used in all beam-to-column connection joints.

2. To identify the effects of connections initial and post-yield stiffness on the joint unloading behavior of semi-rigid frame. The connection unloading would cause in some member internal force redistribution that needs to be incorporated in the design process.

Also, it is highly recommended that this algorithm be expanded to incorporate general dynamic loadings on 3-D semi-rigid frames. In particular, the effects of earthquake induced load ground motion acceleration, is recommended to be implemented in the developed program.

REFERENCES

[1] Chan, S.L., Chui, P.P.T., Non-Linear Static and Cyclic Analysis of Steel Frames With Semi-Rigid Connections, Elsevier, Netherlands, 2000.

[2] Willems and Lucas, Matrix Analysis for Structural Engineers, Prentice-Hall, NJ, 1968.

Hall, Arthur S., Woodhead, Ronald W., Frame Analysis, 2/e, Robert E. Krieger Publishing Company, NY, 1980.

Chen, W.F., Lui, E.M., Stability Design Of Steel Frames, Boca Raton Ann Arbor Boston London.

Semi-Rigid Connections In Steel Frames, Council on Tall Buildings And Urban Habitat.

Y. B. Yang., S. R. Kuo., Theory & Analysis of Nonlinear Framed Structures, Printice Hall, New York, London.

Gill, Dudley W., Building Web Applications with C# and . Net., Boca Raton London New York Washington, D. C..

Deitel Developr Series, C# for Experienced programmers., Prentice Hall, Upper Saddle River, New Jersey 07458.

Holzer, Siegfried M., Computer Analysis of Structures, Matrix Structural Analysis, Structured Programming, Elsevier, New York, 1985.

R. Narayanan, Steel Framed Structures, Stability and strength, Elsevier Applied Science Publishers Inc., London and New York, 1985.

Fertis, Demeter G., Nonlinear Mechanics, CRC Press, Florida, 1993.

Chen, W.F., Goto, Yoshiaki, Liew, J.Y. Richard, Stability Design of Semi-Rigid Frames, John Wiley & Sons Inc., New York, 1996.

Weaver, William JR., Gere, M. James, Matrix Analysis of Framed Structures (2nd ed.), D. Van Nostrand Company, New York, 1980.

Robert B. Dunaway., Visual Studio .Net., No Strach Press ,San Francisco

Fritz Onion. , Essential ASP.NET with Examples in C#, Addison-Wesley.

Annesha Bakharia. ,Microsoft C# fast and easy web development., Premier Press.

Mojica, J., C# Web Development With ASP.NET: Visual Quickstart Guide, Peachpit Press, 2003.

Tapadiya, P., .NET Programming: A Practical Guide Using C#, Prentice Hall PTR, 2002.

Hojjat Adeli., H.Kim., Web-based Interactive Courseware for Structural Steel Design Using Java., Computer –Aided Civil And Infrastructure Engineering 15, 2000, 158-166.

S.Moni., Donald W. White., Frame View: Object-Oriented Visualization System For Frame analysis., Journal of computing in civil engineering /oct.1996., 276-285.

Abdalla., J.A., C.John Yoon., Objected oriented Finite Element and Graphics Data-Translation Facility., Journal of computing in civil engineering, V.6, No.3,Jul 1992, 302-347.

Kirchner, I., Interactive Graphical Input-Output Systems for FEM Plate Bending Programs, Microcomputers in civil Engineering, 8, 1993, 97-103.

Choi, C., Chung, G., Refined Three-Dimensional Finite Element Model for End-Plate Connection, Journal of Structural Engineering, Nov 1996, 1307-1316.

Gharpuray, V., Aristizabal-Ochoa, J, Simplified Second-Order Elastic-Plastic Analysis of Frames, Journal of Computing in civil engineering, V. 3, No. 1, Jan 1989.

<http://www.siggraph.org/education/materials/HyperGraph/viewing/view3d>

<http://www.mtsu.edu/~csjudy/planeview3D/tutorial-parallel.html>